IFE/KR/E – 2010/001

THE EXTENSION OF THE VØRING MARGIN (NE ATLANTIC) IN CASE OF DIFFERENT DEGREES OF MAGMATIC UNDERPLATING

Institute for Energy Technology

	KJELLER	HALDEN
Address	NO-2027 Kjeller, Norway	NO-1751 Halden, Norway
Telephone	+47 63 80 60 00	+47 69 21 22 00
Telefax	+47 63 81 55 53	+47 69 21 22 01

Report number

IFE/KR/E-2010/001

Date

06/22/10

Report title and subtitle

The extension of the Vøring margin (NE Atlantic) in case of different degrees of magmatic underplating

Number of pages

40

Project/Contract no. and name

ISSN

0333-2039

Client/Sponsor Organisation and reference

ISBN

978-82-7017-811-7 (printed)
978-82-7017-812-4 (electronic)

Abstract

The nature of the Lower Crustal Body (LCB) underneath the western part of the Vøring margin (NE Atlantic) is studied with three scenarios of its extension history: (a) The LCB is Caledonian crust. (b) Half the LCB is Caledonian crust and the other half is emplaced as magmatic underplating in Late Paleocene. (c) The entire LCB is emplaced as magmatic underplating. The extension of the margin transect is obtained with a procedure that accounts for the extension and thinning of the sedimentary basins. This procedure has been extended to include magmatic underplating. The lithosphere is modeled with deposition of sediments and four rift phases since the Early Devonian until today. The forward modeling is mass conservative and the present-day thicknesses of the formations, crust, LCB and magmatic underplate are reproduced. The state of the lithosphere and the sedimentary basins are shown and compared at the beginning and at the end of the rift phases. It is concluded that the scenario with the LCB as only underplating requires an unrealistic amount of extension. A scenario where underplating accounts for maximum half the LCB is more likely. Two different interpretations for the Moho underneath the Utgard High are tested: one with a shallow base-crust and another with a deeper and flatter base-crust. Tectonic modeling of the two versions favors the latter interpretation. The modeling shows that the Late Jurassic rift phase was much more prominent than the Late Cretaceous and Paleocene rift phase for all cases of underplating. A strong Late Jurassic rift phase is consistent with the accumulation space needed for the thick Cretaceous formations. There is no observations of magmatism from the Late Jurassic, although this rift phase is stronger than the Cretaceous and Paleocene rift phase.

FiG (3)

Keywords: Lower crustal body, underplating, lithospheric extension, crustal thinning, beta-factor

	Name	Date	Signature
Author(s)	Magnus Wangen	30/6-2010	Magnus Wangen
Reviewed by	Ingar Johansen	30/6-2010	Ingar Johansen
Approved by	Harald Johansen	30/6-2010	Harald Johansen

The extension of the Vøring margin (NE Atlantic) in case of different degrees of magmatic underplating

Magnus Wangen [a,1], Rolf Mjelde [b] and Jan Inge Faleide [c]

[a] *Institute for Energy Technology P.O.Box 40, N-2027 Kjeller, Norway*

[b] *University of Bergen, Dept. for Earth Science Allegt. 41, N-5007 Bergen, Norway*

[c] *University of Oslo, Dept. of Geosciences, P.O. Box 1047, Blindern N-0316 Oslo, Norway*

Abstract

The nature of the Lower Crustal Body (LCB) underneath the western part of the Vøring margin (NE Atlantic) is studied with three scenarios of its extension history: (a) The LCB is Caledonian crust. (b) Half the LCB is Caledonian crust and the other half is emplaced as magmatic underplating in Late Paleocene. (c) The entire LCB is emplaced as magmatic underplating. The extension of the margin transect is obtained with a procedure that accounts for the extension and thinning of the sedimentary basins. This procedure has been extended to include magmatic underplating. The lithosphere is modeled with deposition of sediments and four rift phases since the Early Devonian until today. The forward modeling is mass conservative and the present-day thicknesses of the formations, crust, LCB and magmatic underplate are reproduced. The state of the lithosphere and the sedimentary basins are shown and compared at the beginning and at the end of the rift phases. It is concluded that the scenario with the LCB as only underplating requires an unrealistic amount of extension. A scenario where underplating accounts for maximum half the LCB is more likely. Two different interpretations for the Moho underneath the Utgard High are tested: one with a shallow base-crust and another with a deeper and flatter base-crust. Tectonic modeling of the two versions favors the latter interpretation. The modeling shows that the Late Jurassic rift phase was much more prominent than the Late Cretaceous and Paleocene rift phase for all cases of underplating. A strong Late Jurassic rift phase is consistent with the accumulation space needed for the thick Cretaceous formations. There is no observations of magmatism from the Late Jurassic, although this rift phase is stronger than the Cretaceous and Paleocene rift phase.

Key words: lower crustal body, underplating, lithospheric extension, crustal thinning, beta-factor

---

[1] Corresponding author. E-mail: Magnus.Wangen@ife.no, tel: +47-6380-6259, fax: +47-6381-5553

1 Introduction

The Vøring margin is a passive volcanic margin off-shore mid-Norway in the NE Atlantic, which has gone through a history of several rift phases. The last rift phase ended with continental breakup and sea-floor spreading in the Early Tertiary. Continental breakup was associated with high rates of magma generation and flood basalts. The western part of the margin is characterized by a high velocity layer ($V_p = 7.2$ to 7.6 km/s) in the lower crust (Planke et al., 1991; Mjelde et al., 1997, 1998). The origin of this high velocity Lower Crustal Body (LCB) is debated. It has been suggested to be magmatic underplating associated with the continental breakup in the early Tertiary (Skogseid et al., 2000). However, the assumption of magmatic underplating as the origin of the entire Lower Crustal Body (LCB) has been unestablished, and other possibilities have been discussed; like a "Tertiary" core complex model, a serpentinisation model and a retrograde, high-grade rocks model (Gernigon et al., 2006).

The purpose of this paper is to test three possibilities regarding the LCB by modeling the following three scenarios of the lithospheric extension history of the Vøring margin: (a) The LCB is an integral part of the old (Caledonian) crust during the entire geohistory. (b) The upper half of the LCB is Caledonian crust and the lower half is magmatic underplating emplaced during continental breakup (c) The entire LCB is breakup related magmatic underplating. The first and third scenarios are the non-magmatic and magmatic end-members, respectively. The second case is an intermediate scenario. It is well established that the Vøring basins are intruded by sills and dikes (Brekke, 2000; Fjeldskaar et al., 2003; Planke et al., 2005). This combined with the fact that large volumes of magma were generated during breakup suggests that the crust is intruded by magma too. But it is not clear if the intrusions and the eventual underplating has had a noticeable impact on the crustal geometry.

The assumption of magmatic underplating has several implications for the geohistory of the margin in terms of extension and subsidence. This paper tries to quantify these implications for the margin's stretching- and subsidence history. The assumption that most (or all) of the LCB is magmatic underplating implies that the continental crust above the LCB must have been substantially thinned prior to continental breakup and magmatism. The question is therefore if the necessary magnitude of the stretching, in case of the underplating hypothesis, is consistent with the thicknesses of the sedimentary formations in the basin. The basins above the LCB have thick Paleozoic sediments which have experienced nearly the entire rifting history of the margin, and it has thick Cretaceous formations which have gone through the late Cretaceous rifting episode. These formations could have been substantially thicker prior to rifting. We present predictions for the paleo-thicknesses of the formations in the Vøring basins for the three scenarios above. These thicknesses can be used to address the likelihood that the LCB is mostly old Caledonian crust or mostly magmatic underplating emplaced in the Paleocene.

There is no unique way to estimate the stretching history of a sedimentary basin. An often used approach is to obtain the tectonic subsidence of the sedimentary basin by the backstripping procedure. The tectonic subsidence can then be compared with the subsidence produced by models for crustal extension and thinning. In this paper we adopt a procedure for estimating the magnitude of crustal extension that also accounts for the extension and the thinning of the sedmentary basin (Wangen and Faleide, 2008). The Vøring Basin has thick formations that have experienced several rift phases, and the thinning of the sediments during the rift-phases has an important impact on the amount of the stretching during each rift phase (Wangen and Faleide, 2008). The procedure for estimating the crustal extension has been improved in order to deal with magmatic underplating. The mass of the magmatic intrusion becomes added to LCB in the numerical grid at a constant rate during the time interval of underplating.

A large amount of seismic data has been collected for the Vøring margin (Eldholm and Ewing, 1971; Bukovics and Ziegler, 1985; Eldholm and Mutter, 1986; Skogseid and Eldholm, 1989; Planke et al., 1991; Skogseid et al., 1992; Digranes et al., 1996; Brekke, 2000), and the present study is based on a transect that has recently been studied by Wangen et al. (2008). There are uncertainties associated with the seismic interpretations of the transect, and two interpretations of the Moho underneath the Utgard High are modeled with respect to possible tectonic implications.

This paper is organized as follows: The extension history of the Vøring margin is discussed, followed by a presentation of the LCB. It is shown how the extension history of the transect is computed, and the estimates for the initial thickness of the crust are presented. The modeled extension history of the transect for the three scenarios of underplating are compared and discussed, together with the two interpretations of the Moho. The extension of the margin is discussed in relation to magmatism and breakup.

2 The extension history of the Vøring margin

The Vøring margin, situated off-shore mid-Norway, is a part of the North-Atlantic passive volcanic margin. It is one of three main segments on the mid-Norwegian margin, which are the Møre, Vøring and the Lofoten margins. The Vøring margin is separated from the Møre margin to the south by the Jan Mayen Lineament and to the north by the Bivrost lineament (figure 1).

The margin developed through a series of rift phases since the Caledonian orogeny, where the last rift phase ended with continental breakup and sea-floor spreading in the Early Tertiary. Extension commenced in the Early Devonian (Andersen and Jamtveit, 1990; Fossen, 2000) and was followed by a rift phase in the Late Carboniferous to Early Permian (Blystad et al., 1995), which created accommodation space for Triassic sediments that cover nearly the entire margin transect (figure 2 and 3). A Late Jurassic rift phase then led to major faulting and reactivation of older fault zones (Skogseid and Eldholm, 1989) in the western part of the margin, which formed deep Cretaceous sub-basins – a characteristic feature of the margin (see figures 2 and 3). This rift phase was substantial west of the Nordland Ridge, but weak to the east along the Trøndelag Platform (figures 2 and 3). The last phase of extension took place in the Late Cretaceous - Early Paleocene and ended with continental breakup and sea-floor spreading.

The breakup period was associated with large igneous activity that covered the outer margin with flood basalts. Also the Vøring basin was intruded by sills (Brekke, 2000; Planke et al., 2005), and the concentration of sills appears to be highest in the central part of the basin where the LCB is thickest (Mjelde et al., 2008). Seismic data interpreted as wrench fractures are suggested as the loci of feeder dikes (Mjelde et al., 2008). The sills are found at deep stratigraphic positions towards the east, which suggests that the sills are fed from dikes in the central part of the basin (Brekke, 2000). Substantial volumes of magma could also have underplated or intruded the lower crust and thereby formed the LCB. It has been suggested that the LCB is entirely magmatic underplating (Skogseid et al., 1992; Mjelde et al., 1997), which has been challenged by authors who argue that the LCB represents high-grade rocks from the Caledonies (Gernigon et al., 2003, 2004; Ebbing et al., 2006). These authors also discuss the possibility that the LCB is partly Caledonian crust and partly magmatic underplating. The aim of this paper is to constrain the fraction of magmatic intrusives that may constitute the LCB.

The cause for the voluminous igneous activity during continental breakup is also debated. The Iceland mantle plume has therefore been invoked to explain the magma generation and the flood basalts (White, 1988; Campbell, 2007; Condie, 2001), which provides sufficiently high mantle potential temperatures. Alternatives to a mantle plume have been suggested, as for instance the upwelling of high fertility mantle (Foulger and Anderson, 2005) or small scale mantle convection (Mutter et al., 1988; Boutilier and Keen, 1999). It should be noted that a mantle plume, magma generation and volcanism are not included in the modeling presented here. The magma that underplates (intrudes) the lower crust is simply emplaced at a constant rate during a fixed time interval. The thermal transients from underplating are not discussed in this study, which is restricted to the origin of the LCB and the tectonic development of the margin.

The modeling is based on the following four rift phases: (1) Devonian 400 Ma – 360 Ma, (2) Permian 310 Ma – 260 Ma, (3) Late Jurassic 160 Ma – 146 Ma and (4) Late Cretaceous-Paleocene 80 Ma – 56 Ma, which cover the entire extension history of the basin. These rift phases have been used in earlier attempts to model the extension history of the Vøring margin (Skogseid et al., 1992, 2000; Reemst and Cloetingh, 2000; Gomez et al., 2004; Kuznir et al., 2005; Gernigon et al., 2006; Wangen et al., 2008).

There have not been many attempts to model the tectonic implications of underplating at a volcanic margin. Gernigon et al. (2006) has presented several simulation cases for the Vøring margin which include lithospheric extension, magma generation by decompression melting and underplating. Fjeldskaar et al. (2003) has modeled the thermal transients from underplating and their implications for maturation of source rocks.

3 The Lower Crustal Body (LCB)

The LCB, which is characterized by P-velocities between 7.2 and 7.6 km/s, is mapped under large parts of the western side of the Vøring margin (figures 2 and 3). These velocities are representative of mafic rocks and have been interpreted as magmatic underplating associated with the final stage of rifting, continental breakup and the on-set of sea-floor spreading, (White and McKenzie, 1989; Cox, 1993; Rutter et al., 1993; Thybo et al., 2000). This view has recently been challenged by (Gernigon et al., 2004, 2006), who discuss different alternatives for the origin of the LCB, which are: (1) A mafic-ultramafic model where magmatism is triggered by a mantle plume; (2) A Tertiary core complex model; (3) A serpentinization model and (4) A retrograde, high-grade rock model.

Gernigon et al. (2004) have studied the LCB below the Northern Gjallar Ridge (NGR). An interesting feature of the NGR concerns a mid-crustal dome-shaped reflection, underlying the ridge (Gernigon et al., 2006). The reflection has been regionally mapped and named the T-Reflection (Gernigon et al., 2003, 2004). Recent investigations suggest that the T-Reflection coincides with the top of the continental part of LCB. This part of the LCB imaged beneath the NGR appears to have been in place before the main volcanic event (Gernigon et al., 2006). This structure influenced the development of the sedimentary basin at least 10 Myr to 15 Myr before breakup. Gernigon et al. (2006) conclude that the continental part of the LCB observed beneath the outer Vøring Basin may be partly (or fully) attributed to inherited, high-pressure granulite/eclogite lower crustal rocks. The amount of magmatic material emplaced along the Vøring margin could therefore be much less than earlier assumed.

Mjelde et al. (2008) concludes that the LCB in the continental part of the margin is most likely mafic rocks intruded during the last stage of continental rifting, but it is not ruled out that the LCB might represent an older mafic body. The alternative models for the LCB are not applied within the continental-ocean transition, which is considered as mafic rocks.

There is no evidence of magmatism older than Early Eocene in the Vøring Basin. Magmatic activity is mainly constrained by well ODP site 642E on the Vøring marginal high that drilled two volcanic intervals. The upper interval consists of Early Eocene basaltic layers, which is related to the breakup. In the modeling underplating takes place in the time interval from 58 Ma to 56 Ma, which is prior to breakup at ~ 55 Ma.

The interpretation of the crystalline basement underneath the Utgard High is uncertain. Two versions of the transect are modeled in an attempt to test their tectonic implications. The first version interprets Moho as the top mantle, which makes the crust thin underneath Utgard High. The second version interprets the Moho as the top of a lower crustal eclogite as in the North Sea and in the southern Vøring Basin (Christiansson et al., 2000; Raum et al., 2006). The latter version has a rather flat base of the crust under most of the Naagrind Syncline and the Træna Basin. Figures 2 and 3 show these two interpretations of the crust. Notice that Moho is defined by velocities from ocean bottom seismographs (OBS) data as a seismic boundary. It is normally interpreted as top (peridotitic) mantle, or as in the latter version under the Utgard High, as top eclogite in the lower crust.

The transect is modeled by a finite element grid of quadrilateral elements organized as columns that follow the extension of the profile (Wangen et al., 2008; Wangen and Faleide, 2008). The magmatic underplating is represented by almost void elements until the beginning of emplacement. These elements have initially 1 m of rock before they are intruded by magma. Mass and heat fill these elements during the period of underplating. The magmatic intrusion is by a constant rate at each lateral position in such a way that the observed thickness of the LCB becomes reproduced.

4 Determination of the crustal thinning

Crustal extension is usually obtained from the tectonic subsidence of the sedimentary basin. Tectonic subsidence is the subsidence of the corresponding water filled basin, where for instance Airy isostasy is applied to replace the load of the sediments (and the water above) with the corresponding water load (Allen and Allen, 1990). The tectonic subsidence can be matched with the subsidence from a model of crustal extension and thinning (McKenzie, 1978; Jarvis and McKenzie, 1980). The amount of thinning of the crust is measured by the β-factor, which is the ratio $\beta = c_0/c_1$ of the initial thickness of the crust c_0 over the thickness of the stretched crust c_1. It also measures the amount of extension in a column of lithospheric rock that is thinned by a factor β.

A problem with the backstripping procedure is that is does not account for the extension and thinning of the sedimentary basin. This is in particular a problem for the deep sub-basins of the Vøring margin because the margin has gone through a history of several rift phases with a substantial amount of rifting. Especially the thick Paleozoic sediments, but also several of the thick Cretaceous formations, have experienced rifting with substantial extension. A procedure for estimating the amount of stretching (β-factors), which conserves the mass of the sedimentary basin and the crust during the extension process, has recently been suggested by Wangen and

Faleide (2008). The large scale deformations along normal faults for a wide basin transect are approximated by pure shear deformations, which is a simple continuum description of the stretching process. The procedure assumes that the intervals between the different rifting phases are sufficiently long for thermal uplift to become negligible. The pure-shear assumption allows for a simple estimate of the β-factors that accounts for the extension and thinning of the sedimentary formations in a mass conservative manner. The appendix gives a summary of this procedure.

The tectonic subsidence and the β-factors depend on the paleo-water depth for which there are no standard procedures to obtain. It is often estimated on the basis of the both micro-paleontological and structural observations in combination with tectonic modeling. The paleo-water remains highly uncertain and can often only discriminate against shallow water and deep water. The applied paleo-water in this study is the same as in Wangen et al. (2008), which is an updated version of the paleo-water depth suggested by Kjennerud and Sylta (2001). The uncertainties in the β-factors due to the uncertainties in the paleo-water depth are studied in Wangen and Faleide (2008), who concluded that reasonable differences in the paleo-water depth do not change the conclusions. In particular, the total (or accumulative) stretching remains unchanged for different estimates of the paleo-water depth as long as the present day water depth is the same.

5 The initial crustal thickness and underplating

The computation of crustal stretching in terms of β-factors requires knowledge of the initial thickness of the crust. The thickness of the crust at the beginning of the geohistory can be estimated using data for the present-day sediment depth of the basin (s_{N+1}) and the present-day water depth (w_{N+1}). The assumption of isostasy then gives the initial thickness

$$c_0 = c_{N+1} + f_w(w_{N+1} - w_0) + f_{N+1} s_{N+1} \tag{1}$$

where the w_0 is the water depth at the beginning of the geohistory. The initial water depth w_0 is set to zero in the following. The factors

$$f_w = \frac{\varrho_m - \varrho_w}{\varrho_m - \varrho_c} \quad \text{and} \quad f_{N+1} = \frac{\varrho_m - \varrho_{N+1}}{\varrho_m - \varrho_c} \tag{2}$$

are expressed with the mantle density $\varrho_m = 3300$ kg m^{-3}, the average crustal density $\varrho_c = 2800$ kg m^{-3}, water density $\varrho_w = 1000$ kg m^{-3} and the present-day average basin sediment density ϱ_{N+1}. The sediment density density is the average $\varrho_{N+1} = (1 - \phi_a)\varrho_s + \phi_a \varrho_w$, where $\varrho_s = 2650$ kg m^{-3} is sediment grain density and ϕ_a is the average basin porosity. The initial thickness of the crust (1) gives right away the maximum (present-day) crustal thinning

$$\beta_{\max} = \frac{c_0}{c_{N+1}} = 1 + f_w \frac{w_{N+1}}{c_{N+1}} + f_{N+1} \frac{s_{N+1}}{c_{N+1}} \tag{3}$$

which applies for a column of rock in the lithosphere. The lithosphere along the transect is approximated by a row of such columns. Each column spans the entire lithosphere in the vertical direction, (sedimentary basin, crust and lithospheric mantle), and it deforms by pure-shear during an extension phase with its own strain-rate. Deformation by pure shear assures that the vertical sides of the columns remain vertical during extension. The use of vertical columns is a common approach in modeling lithospheric extension processes (Skogseid et al., 2000; Reemst and Cloetingh, 2000; Gernigon et al., 2006; Wangen et al., 2008).

We now want to make three following models for the extension history of the Vøring margin: (a) The LCB is a part of the crust during the entire basin history. (b) The upper half of the LCB is Caledonian crust and the lower half is emplaced as underplating during continental breakup in the Late Paleocene. (c) The entire LCB is emplaced as underplating during breakup. We need the initial thickness of the crust for each of these three scenarios of the Vøring margin with respect to underplating.

Increasing the thickness of the crust leads to uplift. Airy isostasy implies that the addition of a crustal thickness c_{UP} gives an uplift $w_{\mathrm{UP}} = c_{\mathrm{UP}}/f_w$. We have that $f_w \approx 5$ and, for example, the crustal addition $c_{\mathrm{UP}} = 5$ km therefore gives 1 km of uplift. The initial crustal thickness (1) can be rewritten as

$$c_0 = c'_{N+1} + c_{\mathrm{UP}} + f_w(w'_{N+1} - w_{\mathrm{UP}} - w_0) + f_{N+1} s_{N+1} \tag{4}$$

when the effect of magmatic underplating is taken out as separate parts of the crust and the water depth. The present-day thickness of the crust c_{N+1} is the sum of the thickness of the underplate c_{UP} and the thickness of the Caledonian crust c'_{N+1}. The present-day water depth w_{N+1} is written, in a similar way, as the water depth in the absence of the underplate w'_{N+1} minus the uplift from the underplate w_{UP}. The increased water depth w_{UP} compensates exactly for the thickness of the underplate c_{UP} in equation (4). We therefore let the initial thickness of the crust be independent of the amount of magmatic underplating in the LCB.

Figure 2a shows the transect with basin and basement, where the horizons and the Moho are the same as in a recent study of the Vøring margin (Wangen et al., 2008). Figure 2b shows both the present-day thickness of the crust and an estimate of its initial (Devonian) thickness. The present-day crustal thickness is substantially thinner beneath the Vøring basins west of the Utgard High than beneath the Helgeland Basin to the east. It increases from less than 10 km underneath western part of the transect (between Hel Graben and Træna Basin) to roughly 20 km underneath the Trøndelag platform on the eastern side of the transect. The initial (Early Devonian) thickness of the crust is roughly ~ 30 km to the west of the Utgard High and it increases to ~ 35 km towards the East. There is a minimum in the initial thickness at the present-day position of the Utgard High.

Figure 3 shows the alternative version of the transect where the base crust is deeper and flatter underneath the Utgard High. The basis for this new interpretation is that a body underneath the Moho at this position is eclogite, which therefore becomes a part of the initial crust. The eclogite interpretation is similar to an interpretation applied in the southern part of the Vøring Basin (Mjelde et al., 2008). The shallower Moho underneath Utgard high of the first version could be related to a large detachment fault, an interpretation that has been applied to explain the shallow Moho underneath the Lofoten Ridge further North. The tectonic modeling allows us to compare these two interpretations of the crust underneath the Utgard Ridge. The two bodies, the LCB and the eclogite, of the version with a deeper crust end at the Fles Fault Complex (FFC), which might suggest that the FFC is the Caledonian main suture. The FFC is a zone of weakness that has been active during the long tectonic history of the Norwegian margin (Dore et al., 1997).

Figure 3b shows that the estimate for the initial thickness of the crust is smoother for the version with a deeper and flatter base of the crust underneath the Utgard High. The minimum in the initial crustal thickness at the position of Utgard High is reduced, and it has an average thickness that is ~ 35 km. A constant thickness for the initial crust has been the common assumption in most studies of the extension history of the Vøring margin. Reemst and Cloetingh (2000); Kuznir et al. (2005); Gernigon et al. (2006) all use an initial crust with a thickness of 35 km.

6 Comparison of lithospheric extension: LCB as underplating and LCB as old crust

Figure 4 shows the version with a shallow base of the crust underneath the Utgard High. The figure shows the crustal thickness for the three scenarios of underplating, when the magmatic underplates are subtracted. This is therefore the thickness of the crust at Late Paleocene just prior to magmatic underplating. It is assumed that most of the Late Cretaceous – Paleocene rifting have taken place before underplating at the time of breakup. The initial thickness of the crust is the same for all three scenarios. But the thickness of the crust prior to underplating is nearly half as thin underneath the Naagrind Syncline for the scenario where the entire LCB is underplating. The total (accumulative) amount of crustal stretching is therefore nearly a factor two larger in this case in the area of the Naagrind Syncline. Therefore, the total stretching becomes considerably larger for the western part of the transect with LCB as magmatic underplating. Figure 5 shows the crust prior to underplating for the version with a deeper and flat base-crust underneath Utgard High.

The applied procedure for estimating the β-factors takes into account the thinning of the basin in addition to the thinning of the crust (Wangen and Faleide, 2008).

This procedure shifts the magnitude of extension for the different rift phases towards Early Devonian time when compared with corresponding results from the backstripping procedure. Especially the Devonian and Late Jurassic rift phases become more important, and the Late Cretaceous – Paleocene rift phase becomes less pronounced, when compared with backstripping (Wangen and Faleide, 2008). However, the total (cumulative) β-factor, which is the product of the β-factors for each rift phase, is the same for both approaches.

Figure 6 shows the β-factors for the version with a shallow base-crust underneath the Utgard High. The three scenarios of underplating are compared, and the β-factors increase with increasing amount of underplating. Especially the Devonian rift phase and the Jurassic rift phase have large β-factors. The assumption of the LCB as only underplating leads to unrealistic large β-factors for the Permian rift phase. A reduction of the underplating to half the LCB produces more reasonable stretching factors.

Figure 7 shows the β-factors for the version of a deeper and more flat Moho. We notice that the “spike” in the β-factors in the first rift phase in figure 6a is reduced in figure 7a. The β-factors associated with the deeper and more flat crust appear more realistic than those of the more shallow base-crust. A comparison of figures 6c and 6d with figures 7c and 7d shows that the β-factors for the last two rift phases are only slightly reduced with a deeper crust. A reduction of the underplating to half the thickness of the LCB gives more reasonable stretching factors for this case too. It should be noted that the “spike” in the β-factor could be the result of a weakness of the suggested method to model extension, which does not take into account large detachement planes with simple shear deformation.

Figures 8, 9 and 10 show the evolution of the upper part of the lithosphere through the geohistory. The series of plot are based on the version with a deep and flat base-crust underneath the Utgard High. The state of the basin, crust, the LCB and the upper mantle are shown at the beginning and the end of the rift phases, and at present time. The LCB is old crust in figure 8, which shows how the lithosphere is stretched out 110 km since the beginning of the Permian rift phase until today. Figures 9 and 10 show that the difference is not so large when compared with the two scenarios where the LCB is half underplating and only underplating. The profile is stretched 120 km and 130 km for these two scenarios, respectively.

Sediments are deposited at the basin surface through the geohistory, and they compact as they get buried. The compaction is given by an Athy-type porosity function Athy (1930), where the porosity decreases exponentially with depth z (measured from the basin surface) as $\phi = \phi_0 \exp(-z/z_0)$. The depth z_0 controls when compaction becomes noticeable. The sediments are modeled with just one lithology, which has the surface porosity $\phi_0 = 0.45$ and the compaction depth $z_0 = 1820$ m. The use of an Athy-type porosity function is a common choice in basin analysis (Allen and Allen, 1990). It should be noted that most of the porosity is lost in the upper 4 km of the basin. The basins are therefore dominated by sediments with low porosity since most of the sediments are deeper than 4 km.

The basin part of the transect is shown with the series of plots in figures 11, 12 and 13 for the same time steps as for the lithosphere in figures 8 to 10 – they are shown at the beginning and the end of the rift phases, and at present time. The mass of each formation in the basin is conserved during rifting, and their present-day thicknesses are reproduced. These figures show that past formation thicknesses increases with increasing amount of underplating. The old (Caledonian) part of the present-day crust gets thinner with increasing underplating, which implies more extension as shown by figures 6 and 7. The pre-rift sedimentary formations therefore become thicker too, because they experience stronger extension and thinning. Figure 10 shows that the case where the LCB is only underplating gives a very thick basin at the beginning of the last rift phase in the Late Cretaceous. The case where only half the LCB is underplating gives a more reasonable basin geohistory.

7 Extension, Break-up and magmatism

Our modeling does not cover the continental-ocean transition (COT) and breakup. The COT is not well mapped on volcanic margins because of the thick basaltic cover that limits seismic imaging. Nevertheless, Mjelde et al. (2007) interpret the final rift phase and breakup to be closely related to the development of a crustal scale detachement fault and they defined the COT by means of this detachement fault. The large thickness of the stretched continental crust on the seaward side of the Vøring escarpment is described by Mjelde et al. (2001). Mjelde et al. (2007) points out that the Late Cretaceous/Early Tertiary thinning cannot be explained by pure-shear model with gradually increasing stretching factors until continental breakup occurred. Thinning of the outer Vøring margin is explained by Mjelde et al. (2007) as detachment faults soling out in the lower crust.

Breivik et al. (2009) studied magma productivity along the Vøring margin and pointed out the following observations: (1) There is a strong correlation between magma production and the early plate spreading rate. (2) The magma production peaks at breakup at the mid-Norwegian margin. (3) Magmatism is segmented along the mid-Norwegian margin, since there is considerably less magma production to the northeast along the Lofoten margin and to the south along the Møre margin. Breivik et al. (2009) concluded that these observations may be explained with hot and bouyant material from a mantle plume upwelling from a center underneath Greenland, that flow laterally to pond into the topography of the North Atlantic rift zone.

Figure 6c, 6d, 7c and 7d show that the Late Jurassic rift phase is considerably stronger than the Late Cretaceous and Paleocene rift phase, with β-factors more than twice as large in the tectonic active Western part of the transect. This result follows from the mass conservative procedure for estimating the β-factors as shown by Wangen and Faleide (2008). On the other hand, estimation of the β-factors based on the backstripping procedure gives the opposite result – the Late Cretaceous and Paleocene rift phase becomes more prominent than the Late Jurassic rift phase (Wangen and Faleide, 2008). The results of the new procedure are more reasonable because the Late Jurassic rifting created the accumulation space for the thick Cretaceous formations. The infill of sediments during the Cretaceous took place during the thermal subsidence from the Late Jurassic rifting.

There are no observations of magmatism related to rifting in the Late Jurassic, although this rift phase was considerabley stronger than the Late Cretaceous – Paleocene rift phase for the Western part of the profile. It therefore seems as if the large amount of magmatism and the flood basalts are not explained by extension alone. The magmatism appears to be related to the breakup, the mantle upwelling and the continental separation. None of the often suggested models for the magmatism can easily be ruled out, like for instance a mantle plume (White, 1988; Campbell and Griffits, 1992; Condie, 2001), the upwelling of high fertility mantle (Foulger and Anderson, 2005) or small scale mantle convection (Mutter et al., 1988; Boutilier and Keen, 1999). It should also be mentioned that substantial amounts of magmatism can be produced without any breakup and modest stretching factors as seen in the Oslo rift (Larsen et al., 2008).

8 Conclusion

Three scenarios of the extension history of a transect from the Vøring margin have been studied in order to constrain the possible fraction of magmatic underplating in the LCB. These scenarios are: (a) The LCB is Caledonian crust. (b) Half the LCB is Caledonian crust and the other half is is emplaced as magmatic underplating in Late Paleocene. (c) The entire LCB is emplaced as magmatic underplating.

The extension (the β-factors) of the transect have been obtained using a new procedure that accounts for the thinning of the sedimentary formations during the rift phases. This procedure has been extended to handle magmatic underplating. The pre-rift sedimentary formation thicknesses are obtained and the geohistory of the lithosphere is modeled. The entire lithosphere is extended through the four rift phases of the geo-history in a mass conservative manner, and the present-day thicknesses for sedimentary formations, crust, LCB and eventual underplating are reproduced. The state of the lithosphere and the sedimentary basin are shown and compared for the beginning and the end of the rift phases and at present time.

The scenario where the LCB is underplating implies that the crust over the LCB was quite thin (~ 2.5 km) before intrusion of magma. The cumulative extension after the collapse of the Caledonian orogeny becomes quite large. This is problematic if sedimentary formations like the Paleozoic have experienced a similar amount of extension as the upper crust. These formations must then have been considerable thicker at earlier times. It is therefore concluded that the scenario where the LCB is fully underplating gives too much extension, and it is therefore unlikely. The two other scenarios give more reasonable extension histories, which are not very different from each other, and it is concluded that up to half the LCB may be due to magmatic underplating.

The interpretation of the crust underneath the Utgard High is uncertain. Two different interpretations for the crust are tested: one with a thin crust and another with a deeper and flatter base of the crust. The first of these interpretations corresponds to a detachment fault under the Utgard High, while the version with a deeper base of the crust has a body underneath the Moho being interpreted as eclogite. Tectonic modeling of the two scenarios favors the thick crust interpretation, because a "spike" in the β-factor appears in the version with a shallow crust at the position of the Utgard High. The estimated initial thickness of the crust is also more even.

The β-factors for the late Jurassic rift phase is more prominent than for the late Late Cretaceous – Paleocene rift phase for all three scenarios of underplating. Large β-factors of the late Jurassic rift phase fits the observations, because they are needed to create the accumulation space for the mapped thick Cretaceous formations.

There are no observations of magmatism in the Late Jurassic although this rift phase has considerablely larger β-factors than the Late Cretaceous – Paleocene rift phase for the Western part of the profile. It therefore seems as if the large amount of magmatism and the flood basalts are not only related to extension, but also in some way to the breakup, the mantle upwelling and the continental separation. None of the often sited models for the magmatism can be ruled out, like for instance a mantle plume, the upwelling of high fertility of the mantle lithosphere, or small scale mantle convection.

9 Appendix: β-factors that account for stretching and thinning of the sedimentary basin.

Equation (1) for the initial thickness of the crust can be rewritten as an equation for the thickness of the crust as the following function of time

$$c(t) = c_0 - f_w w(t) - f(t)s(t) \tag{5}$$

where $w(t)$ is the water depth and $s(t)$ is the sediment thickness at the time t. The factor $f(t) = (\varrho_m - \varrho_s(t))/(\varrho_m - \varrho_c)$ replaces the factor f_{N+1} and it has the time-dependent average basin density $\varrho_s(t)$. The cumulative crustal stretching as function of the time becomes

$$\beta_{\max}(t) = \frac{c_0}{c(t)} = \frac{c_0}{c_0 - f_w w(t) - f(t)s(t)} \tag{6}$$

The cumulative amount of crustal stretching at the beginning of each rift phase i becomes

$$\beta_{\max,i} = \beta_{\max}(t_i) \tag{7}$$

which makes the β-factor for this rift phase

$$\beta_i = \frac{\beta_{\max,i+1}}{\beta_{\max,i}} \quad \text{for} \quad i = 1, \dots, N \tag{8}$$

The cumulative stretching is initially $\beta_{\max,1} = 1$, because there is no crustal thinning before the first rift phase, and $\beta_{\max,N+1}$ is the present-day (maximal) β-factor.

A generalization to more or less rift phases is straightforward. The cumulative β-factor at the beginning of the first rift phase is

$$\beta_{\max,1} = 1 \tag{9}$$

because the crust is unstretched until then. At the beginning of the second rift phase (at time t_2) the cumulative β-factor becomes

$$\beta_{\max,2} = \frac{c_0}{c_0 - f_w w_2 - \beta_2\beta_3\beta_4 f_2 s_2} \tag{10}$$

This expression is different from the preceding one by having the thickness of the sedimentary basin increased by the product $\beta_2\beta_3\beta_4$. The sediments deposited until the second rift phase, which has the thickness s_2, must have been a factor $\beta_2\beta_3\beta_4$

thicker, because they have experienced rift phases 2, 3, and 4. Similarly, the cumulative β-factor for the third rift phase is

$$\beta_{\max,3} = \frac{c_0}{c_0 - f_w w_3 - \beta_3 \beta_4 f_3 s_3} \tag{11}$$

because the sediments deposited until the third rift phase, which at present time has the thickness s_3, have gone through rift phases 3 and 4. This thickness was therefore a factor $\beta_3\beta_4$ thicker at the beginning of rift phase 3. At the beginning of the fourth rift phase we have

$$\beta_{\max,4} = \frac{c_0}{c_0 - f_w w_4 - \beta_4 f_4 s_4} \tag{12}$$

and at the present time

$$\beta_{\max,5} = \frac{c_0}{c_0 - f_w w_5 - f_5 s_5} \tag{13}$$

At the same time we have that the β-factor for each rift phase is given by the cumulative β-factor by expression (8). The five equations (9) to (13) and the four equations (8) (i from 1 to 4) are nine equations for the altogether nine unknowns, which are the four β-factors and the five cumulative β-factors. These equations for the β-factors can be solved by the following procedure, where the last β-factor is found first, which is then used to obtain the next last β-factor and so forth. The β-factors in reverse order become

$$\beta_4 = \frac{c_0 - f_w w_4}{c_0 - f_w w_5 - (f_5 s_5 - f_4 s_4)} \tag{14}$$

$$\beta_3 = \frac{c_0 - f_w w_3}{c_0 - f_w w_4 - \beta_4 (f_4 s_4 - f_3 s_3)} \tag{15}$$

$$\beta_2 = \frac{c_0 - f_w w_2}{c_0 - f_w w_3 - \beta_4 \beta_3 (f_3 s_3 - f_2 s_2)} \tag{16}$$

$$\beta_1 = \frac{c_0 - f_w w_1}{c_0 - f_w w_2 - \beta_4 \beta_3 \beta_2 (f_2 s_2 - f_1 s_1)} \tag{17}$$

The last β-factor depends on the difference $f_5 s_5 - f_4 s_4$, which is close to being proportional to the difference $s_5 - s_4$. This difference is the accumulation space needed for sediments that are filled in after the last rift phase. The proceeding β-factors are similarly dependent on the accumulation space needed for the sediments that follow the rift phase, and they are inflated by the β-factors of the rift phases that follow. The β-factor for the first rift phase is therefore dependent on the β-factors of the 2nd, 3rd and 4th rift phase.

10 Acknowledgment

The authors are grateful for the suggestions and corrections to the manuscript made by Yuriy Maystrenko, Ross Boutilier and an anonymous reviewer.

References

ALLEN, P.A. & ALLEN, J.R. (1990) *Basin analysis*. Blackwell Scientific Publications.

ANDERSEN, T. & JAMTVEIT, B. (1990) Uplift of deep crust during orogenic extensional collapse: A model based on field studies in the Sogn-Suffjord Region of western Norway. *Tectonics*,**9**, 1097–1111.

ATHY, L.F. (1930) Density, porosity, and compaction of sedimentary rocks. *AAPG Bulletin*, **14**, 1–22.

BLYSTAD, P., BREKKE, H., FÆRSETH, R.B., LARSEN, B. T., SKOGSEID, J. & TØRUDBAKKEN, B. (1995) Structural elements of the Norwegian continental shelf. *NPD Bulletin 8*, **45**, Norwegian Petroleum Directorate.

BREKKE, H. (2000) The tectonic evolution of the Norwegian Sea continental margin with emphasis on the Vøring and the Møre basins. In: *Dynamics of the Norwegian Margin* (Ed. by A. Nøttvedt), *Geological Society Special Publication*, **167**, 327–378. The Geological Society, London.

BREVIK, A.J., FALEIDE, J.I., MJELDE, R., FLUEH, E.R. (2009) Magma productivity and early seafloor spreading rate correlation on the northern Vøring Margin, Norway – Constraints on mantle melting. *Tectonophysics*, **468**, 206–223.

BUKOVICS, C. & ZIEGLER, P.A. (1985) Tectonic development of the mid-Norway continental margin. *Marine and Petroleum Geology*, **2**, 2–22.

BOUTILIER, R.R. & KEEN, C.E. (1999) Small-scale convection and divergent plate boundaries. *Journal of Geophysical Research*, **104** (B4), 7389–7403.

CAMPBELL, I. & GRIFFITHS, R.W. (1992) The changing nature of mantle hotspots through time: implications for the chemical evolution of the mantle. *Journal of Geology*, **92**, 497–523.

CAMPBELL, I. (2007) Testing the plume theory. *Chemical Geology*, **241**, 153–176.

CHRISTIANSSON, P., FALEIDE, J.I., BERGE, A. (2000) Crustal structure in the northern North Sea: an integrated geophysical study. In: *Dynamics of the Norwegian Margin* (Ed. by A. Nøttvedt), *Geological Society Special Publication*, **167**, 15–40. The Geological Society, London.

CONDIE, K.C. (2001) Mantle plumes and their record in the Earth history. *Cambridge University Press*, Cambridge, England.

COX, K. (1993) Continental magmatic underplating. *Royal Society of London Philosophical Transactions A*, **342**, 155–166.

DIGRANES, P., MJELDE, R., KODAIRA, S., SHIMAMURA, H., KANAZAWA, T., SHIOBARA, H. & BERG, E.W. (1996) Modeling shear waves in OBS data from the Vøring basin (Northern Norway) by 2-d ray-tracing. *Pure and Applied Geophysics*, **147**, 611–629.

DORÉ, A.G., LUNDIN, E.R., FISCHLER, C., & OLSEN, O. (1997) Patterns of basement structure and reactivation along the NE Atlantic margin. *Journal of the Geological Society of London*, **154**, 85–92.

EBBING, J., LUNDIN, E., OLESEN, O. & HANSEN, E. (2006) The mid-Norwegian margin: A discussion of crustal lineaments, mafic intrusions, and remnants of the caledonian root by 3D density modelling and structural interpretation. *Journal of the Geological Society, London*, **163**, 47–59.

ELDHOLM, O. & EWING, J. (1971) Marine geophysical survey in the southwestern Barents Sea. *Journal of Geophysical Research*, **76**, 3832–3841.

ELDHOLM, O. & MUTTER, J.C. (1986) Basin structure of the Norwegian margin from analysis of digitally recorded sonobuoys. *Journal of Geophysical Research*, **91 (B3)**, 3763–3783.

FERNANDEZ, M., AYALA, C., TORNE, M., VERGES, J., GOMEZ, M. & KARPUZ, R. (2005) Lithospheric structure of the mid-Norwegian Margin: comparisons between the Møre and the Vøring Margins. *Journal of the Geological Society, London*, **162**, 1005–1012.

FJELDSKAAR,W., JOHANSEN, H., DODD, T.A. & THOMPSON, M. (2003) Temperature and maturity effects of magmatic underplating in the Gjallar Ridge, Norwegian Sea. In: *Multidimensional basin modeling* (Ed. by S. Dü ppenbecker & R. Marzi) *AAPG/Datapages, Discovery Series*, no. 7, 71–85.

FJELDSKAAR, W., HELSET, H.M., JOHANSEN, H., GRUNNALEITE, I. & HORSTAD, I. (2008) Thermalmodelling ofmagmatic intrusions in the Gjallar Ridge, Norwegian Sea: implications for vitrinite reflectance and hydrocarbon maturation. *Basin Research*, **20**, 143–159.

FOSSEN, H. (2000) Extensional tectonics in Caledonides: Synorogenic or postorogenic? *Tectonics*, **9**, 213–224.

FOULGER, G.R.. & ANDERSON, D.L. (2005) A cool model for the Iceland hotspot. *Journal of Volcanology and Geothermal Research*, **141**, 1–22.

GERNIGON, L., LUCAZEAU, F., BRIGAUD, F., RINGENBACH, J.-C., PLANKE, S. & BERBARD, L. (2006) A moderate melting model for the Vøring Margin (Norway) based on structural observations and thermo-kinematical modeling: Implication for the meaning of the lower crustal body. *Tectonophysics*, **412**, 255–278.

GERNIGON, L., RINGENBACH, J.C. & PLANKE, S. (2003) Extension, crustal structure and magmatism at the outer Vøring Basin, North Atlantic margin, Norway. *Journal of the Geological Society, London*, **160**, 197–208.

GERNIGON, L., RINGENBACH, J.C., PLANKE, S. & LE GALL, B. (2004) Deep structures and breakup along volcanic rifted margins: insights from integrated studies along outer Vøring Basin (Norway). *Marine and Petroleum Geology*, **21**, 363–372.

GÓMEZ, M., VERGÉS, J., FERNÀNDEZ, M., TORNE, M., AYALA, C., WHEELER, W., & KARPUZ, R. (2004) Extensional geometry of the Mid Norwegian Margin before early Tertiary continental breakup. *Marine and Petroleum Geology*, **21**, 177–194.

JARVIS, G. & MCKENZIE, D. (1980) Sedimentary basin formation with finite extension rates. *Earth and Planetary Science Letters*, **48**, 42–52.

KJENNERUD, T. & SYLTA, O. (2001) Application of quantitative paleobathymetry in basin modeling, with reference to the North Sea. *Petroleum Geoscience*, **7**, 331–341.

LARSEN, B.T., OLAUSSEN, S., SUNDVOLL B., AND HEEREMANS M. (2008) The Permo-Carboniferous Oslo Rift through six stages and 65 million years.

Episodes, **31**, no. 1, 52–58.

KUZNIR, N.J., HUNSDALE, R., ROBERTS, A.M. & ISIMM TEAM (2005) Norwegian margin depth-dependent stretching. In: *Petroleum Geology: North-West Europe and Global Perspectives - Proceedings of the 6th Petroleum Geology Conference* (Ed. by A.G. Dore & B.A. Vining) 767–783. *Geological Society, London*.

MCKENZIE, D. (1978) Some remarks on the development of sedimentary basins. *Earth and Planetary Science Letters*, **40**, 25–32.

MJELDE, R., KODAIRA, S., SHIMAMURA, H., KANAZAWA, T., SHIOBARA, H. BERG, E. & RIISE, O. (1997) Crustal structure of the central part of the Vøring basin, mid-Norway margin, from ocean bottom seismographs. *Tectonophysics*, **277**, 235–257.

MJELDE, R., DIGRANES, P., SHIMAMURA, H., SHIOBARA, H., KODAIRA, S., BREKKE, H., EGEBJERG, T., SØRENES, N., THORBJØRNSEN, S. (1998) Crustal structure of the northern part of the Vøring Basin, mid-Norway Margin, from wide-angle seismic and gravity data. *Tectonophysics*, **293**, 175–205.

MJELDE, R., DIGRANES, P., VAN SCHAACK, M., SHIMAMURA, H., SHIOBARA, H., KODAIRA, S., NAESS, O., SØRENES, N. & VÅGNES, E. (2001) Crustal structure of the outer Voring Plateau, offshore Norway, from ocean bottom seismic and gravity data. *Journal of Geophysical Research*, **106**, B4, 6769–6791 .

MJELDE, R., RAUM, T., MURAI, Y. & TAKANAMI, T. (2007) Continent-ocean-transitions: Review, and a new tectono-magmatic model of the Vøring Plateau, NE Atlantic. *Journal of Geodynamics*, **43**, 374–392.

MJELDE, R., FALEIDE, J., BREIVIK, A. & RAUM, T. (2008) Lower crustal composition and crustal lineaments on the Vøring Margin, NE Atlantic. *Tectonophysics*, accepted for publication.

OSMUNDSEN, P.T., SKILBREI, J. & OLESEN, O. (2002) Deep structure of the mid Norway rifted margin. *Norwegian Journal of Geology*, **82**, 205–224.

MUTTER, J.C., BUCK, W.R.. & ZEHNDER, C.M. (1988) Convective partial melting; 1, a model for the formation of thick basaltic sequences during the initiation of spreading. *Journal of Geophysical Research*, **93** (B2), 1031–1048.

PLANKE, S., SKOGSEID, J., ELDHOLM, O. (1991) Crustal structure of Norway, 62^o to 70^o N. *Tectonophysics*, **189**, 91–107.

PLANKE, S., RASMUSSEN, T., REY, S. & MYKLEBUST, R. (2005) Seismic characteristics and distribution of volcanic intrusions and hydrothermal vent complexes in the Vøring and Møre basins. In: *Petroleum Geology: North-West Europe and Global Perspectives - Proceedings of the 6th Petroleum Geology Conference* (Ed. by A.G. Dore & B.A. Vining) 833–844. *Geological Society, London*.

RAUM, T., MJELDE, R., SHIMAMURA, H., MURAI, Y., BRÅSTAIN, E., KARPUZ, R., KRAVIK, K. & KOSTØ, H. (2006) Crustal structure and evolution of the southern Vøring Basin and Vøring Transform Margin, NE Atlantic. *Tectonophysics*, **415**, 167–202.

REEMST, P. & CLOETINGH, S. (2000) Polyphase rift evolution of the Vøring margin (mid-Norway): Constraints from forward tectonostratigraphic modeling. *Tectonophysics*, **19**, 225–240.

References

RUTTER, E., BRODIES, K. & EVANS, P. (1993) Structural geometry, lower crustal magmatic underplating and lithospheric stretching in the Ivrea-Verbano zone, northern Italy. *Journal of Structural Geology*, **15**, 647–662.

SKOGSEID, J. & ELDHOLM, O. (1989) Vøring Plateau continental margin: seismic interpretation, stratigraphy and vertical movements. In: *Proceedings of the Ocean Drilling Program, Scientific Results* (Ed. by O. Eldholm, J. Thiede & E. Taylor), 993–1030. *Ocean Drilling Program, College Station, TX.*

SKOGSEID, J., PEDERSEN, T. & LARSEN, B. (1992) Vøring basin: Subsidence and tectonic evolution. In: *Structural and tectonic modelling and its application to petrolem geology.* (Ed. by R.M. Larsen) *Norwegian Petroleum Society, Special Publications*, 55–82.

SKOGSEID, J., PLANKE, S., FALEIDE, J.I., PEDERSEN, T., ELDHOLM, O. & NEVERDAL, F. (2000) NE Atlantic continental rifting and volcanic margin formation. In: *Dynamics of the Norwegian Margin* (Ed. by A. Nøttvedt), *Geological Society Special Publication*, **167**, 295–326. The Geological Society, London.

THYBO, H., MAGUIRE, P., BIRTH, C. & PERCHUĆ (2000) Seismic reflection and seismic reflectivity and underplating beneath the Kenya Rift. *Geophysical Research Letters*, **27 (17)**, 2745–2748.

WANGEN, M. & FALEIDE, J.I. (2008) Estimation of crustal thinning by accounting for basin stretching and thinning – and example from the Vøring margin, NE Atlantic. *Journal of Tectonophysics*, **457**, 224–238.

WANGEN, M., FJELDSKAAR, W., FALEIDE, J.I., WILSON, J., ZWEIGEL, J. & A., AUSTEGAARD (2008) Forward modeling of stretching episodes and paleo heat flow of the Vøring margin, NE Atlantic. *Journal of Geodynamics*, **45**, 83–98.

WHITE, R.S. (1988) A hot-spot model for early Teriary volcanism in the N. Atlantic. In: *Early Tertiary volcanism and the opening of the NE Atlantic* (Ed. by A.C. Morton & L.M. Parson), *Geological Society Special Publication*, **39**, 295–326.

WHITE, R. & MCKENZIE, D. (1989) Magmatism at rift zones: the generation of volcanic continental margins and flood basalts. *Journal of Geophysical Research*, **94**, no. B6, 7685–7729.

11 Captions

Figure 1 *Profile 2 goes from the Vøring escarpment to almost the Norwegian main land. Structural elements are taken from Blystad et al. (1995); Osmundsen et al. (2002); Mjelde et al. (2008). (VD=Vema Dome, FFC=Fles Fault Complex, RR=Rån Ridge, GL=Gleipne Lineament)*

Figure 2 *(a) The basin part of the transect shows the relatively thick ($\sim$ 5 km) Paleozoic formation at the base, especially under the Trøndelag platform. We also notice the thick Cretaceous formations in the basin to the west of the Trøndelag platform. (b) The crust underneath Træna basin and Westwards is thin ($\sim$ 10 km), and the crust is roughly twice as thick underneath the Trøndelag platform. The high velocity Lower Crustal Body (LCB) is a substantial fraction of the western part of the crust. The initial thickness of the crust has a minimum thickness at the Utgard High.*

Figure 3 *(a) A second version of the crust for the same profile as in figure 2. The crust is deeper and flatter underneath the Utgard High. (b) The estimated initial crustal thickness underneath the Utgard High becomes increased when compared with figure 2.*

Figure 4 *The thickness of the crust at the end of the last (Late Cretaceous - Paleocene) rift phase, immediately before underplating. This figure shows the crust for the three scenarios of the underplating in the case with a shallow base-crust underneath the Utgard High.*

Figure 5 *The thickness of the crust at the end of the last (Late Cretaceous – Paleocene) rift phase, immediately before underplating. The thickness of the crust for the three scenarios of underplating is shown in the case where the crust is deep and more flat underneath the Utgard High.*

Figure 6 *(a) and (b): The β-factors for the first two rift phases (Devonian and Permian) are shown for the three scenarios of underplating, in the case of a shallow base-crust underneath the Utgard High. The scenario where the LCB is only underplating yields considerably larger β-factors than the two other scenarios. (c) and (d): The β-factors for the last two rift-phases (Late Jurassic and Late Cretaceous – Paleocene) are shown for the three scenarios of underplating in the case of a shallow base-crust underneath the Utgard High. The difference between the different scenarios is not as large for the last two rift phases as for the two first.*

Figure 7 *(a) and (b): The same as figure 6a, but in case of the deeper and flatter crust. The "spike" in the β-factors at the position of the Utgard High is considerable reduced when compared with the case of a shallow base-crust in figure 6a. The scenario of underplating yields considerable larger β-factors than the two other scenarios. (c) and (d): The case of a deeper and flatter crust underneath Utgard high has similar β-factors for the two last rift phases as the case with a shallow* *base-crust underneath Utgard High.*

Figure 8 *The scenario where the LCB is Caledonian crust is shown for the case with a deep and flat crust. The upper 40 km of the lithosphere is shown for the beginning and the end of the last three rift episodes and at the present-day.*

Figure 9 *The scenario where the LCB is half Caledonian crust and half underplating is shown for the case with a deep and flat base-crust. The upper 40 km of the lithosphere is shown for the beginning and the end of the last three rift episodes and at the present-day.*

Figure 10 *The scenario where the LCB is entirely underplating is shown for the case with a deep and flat crust. The upper 40 km of the lithosphere is shown for the beginning and the end of the last three rift episodes and at the present-day.*

Figure 11 *The sedimentary basin is shown at the beginning and the end of the last three rift episodes and at the present-day for the scenario with LCB as Caledonian crust. The extension history is for the case of a deep and flat crust.*

Figure 12 *The sedimentary basin is shown at the beginning and the end of the last three rift episodes and at the present-day for the scenario with LCB as half Caledonian crust and half Tertiary underplating. The extension history is for the case of a deep and flat crust.*

Figure 13 *The sedimentary basin is shown at the beginning and the end of the last three rift episodes and at the present-day for the scenario with LCB as Tertiary underplating. The extension history is for the case of a deep and flat crust.*

12 Figures

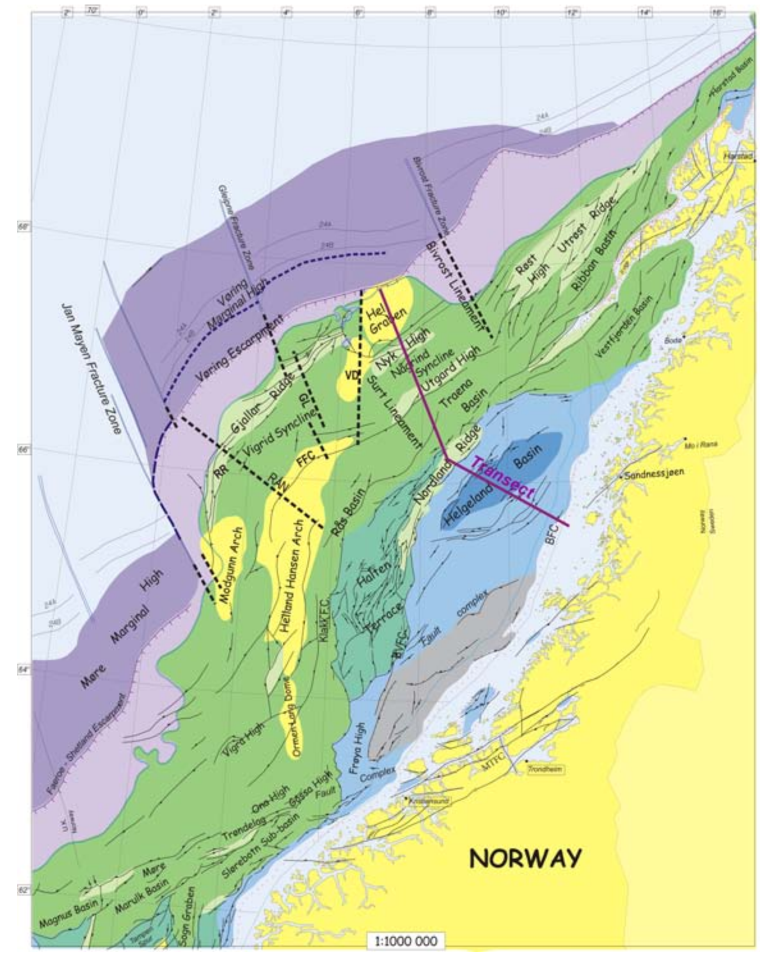
Jan Mayen Fracture Zone
Vøring Marginal High
Vøring Escarpment
Gjallar Ridge
Vigrid Syncline
Bivrost Lineament
Røst High
Utrøst Ridge
Ribban Basin
Vestfjorden Basin
Hel Graben
Nyk High
Någrind Syncline
Utgard High
Træna Basin
Surt Lineament
Nordland Ridge
Helgeland Basin
Transect
BFC
FFC
VD
RR
Rås Basin
Modgunn Arch
Helland Hansen Arch
Klakk FC
Halten Terrace
Fault complex
Møre Marginal High
Vigra High
Ormen Lange Dome
Frøya High
Trøndelag
Slørebotn Sub-basin
Magnus Basin
Marulk Basin
Møre
Sogn Graben
NORWAY
Trondheim
Bodø
Mo i Rana
Sandnessjøen
Harstad
1:1000 000

Figure: 1

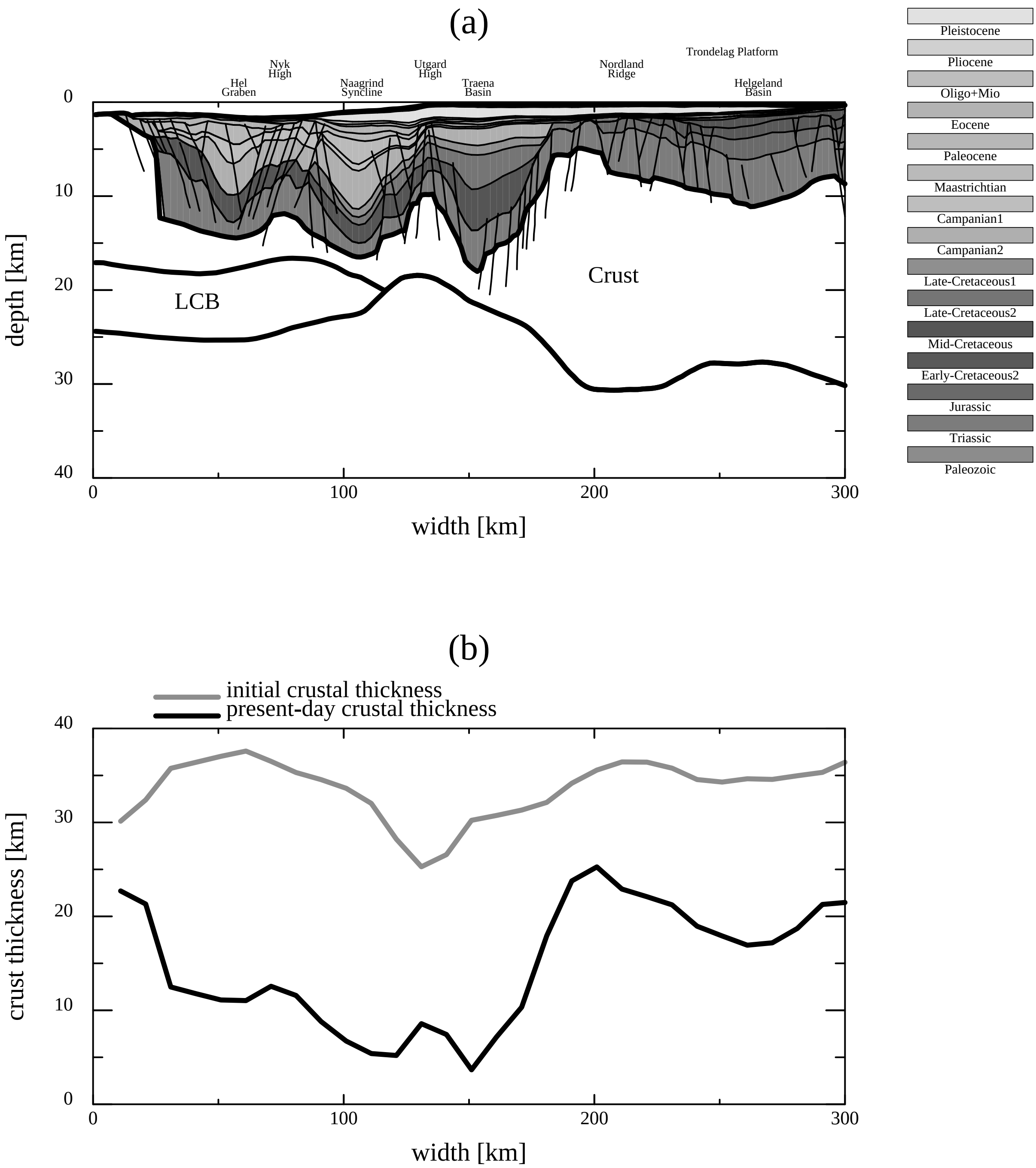

(a)
Pleistocene
Pliocene
Oligo+Mio
Eocene
Paleocene
Maastrichtian
Campanian1
Campanian2
Late-Cretaceous1
Late-Cretaceous2
Mid-Cretaceous
Early-Cretaceous2
Jurassic
Triassic
Paleozoic
Hel Graben
Nyk High
Naagrind Syncline
Utgard High
Traena Basin
Nordland Ridge
Trondelag Platform
Helgeland Basin
Crust
LCB
depth [km]
width [km]
(b)
initial crustal thickness
present-day crustal thickness
crust thickness [km]
width [km]

Figure: 2

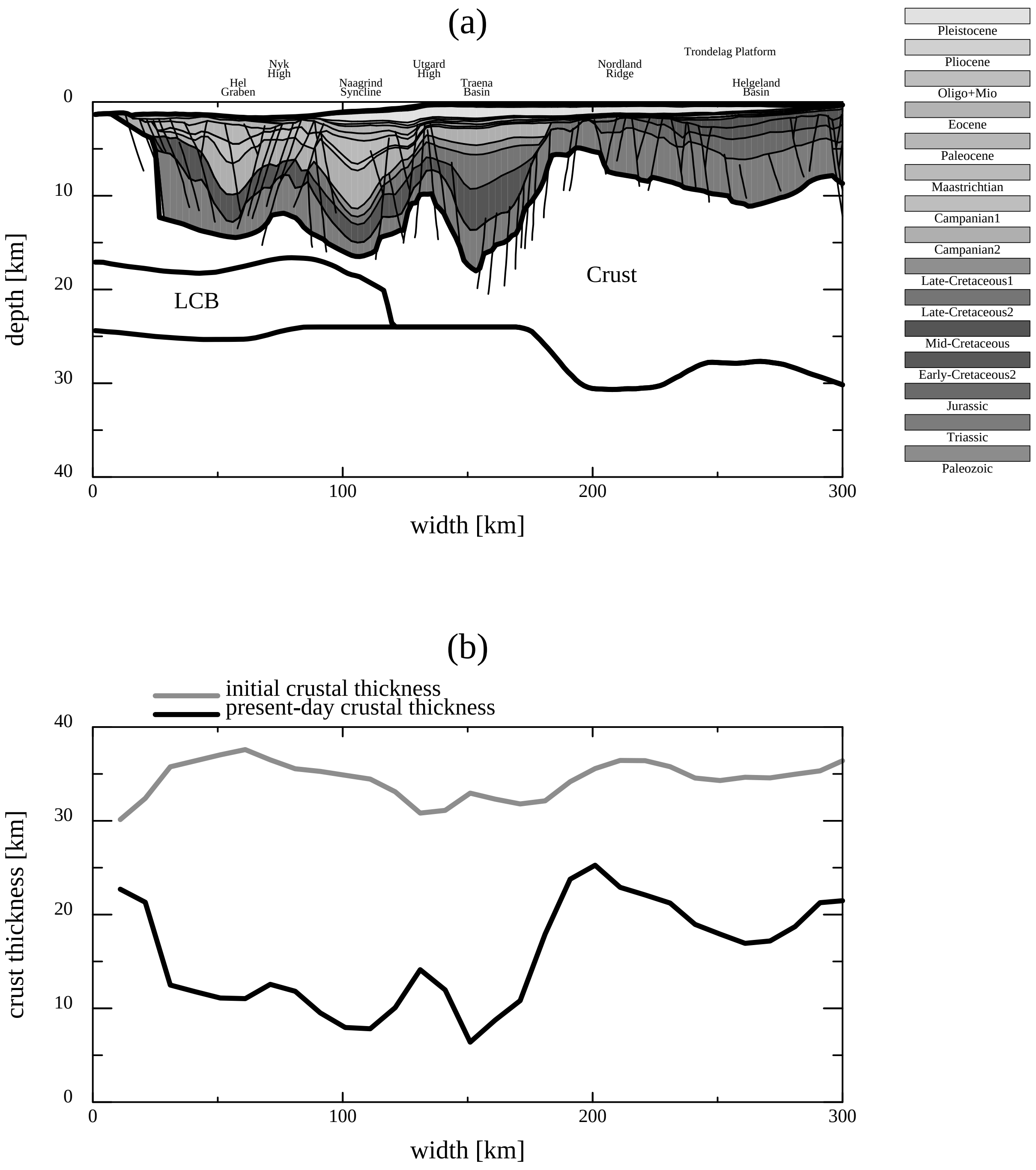

(a)
Hel Graben
Nyk High
Naagrind Syncline
Utgard High
Traena Basin
Nordland Ridge
Trondelag Platform
Helgeland Basin
LCB
Crust
depth [km]
width [km]
Pleistocene
Pliocene
Oligo+Mio
Eocene
Paleocene
Maastrichtian
Campanian1
Campanian2
Late-Cretaceous1
Late-Cretaceous2
Mid-Cretaceous
Early-Cretaceous2
Jurassic
Triassic
Paleozoic
(b)
initial crustal thickness
present-day crustal thickness
crust thickness [km]
width [km]

Figure: 3

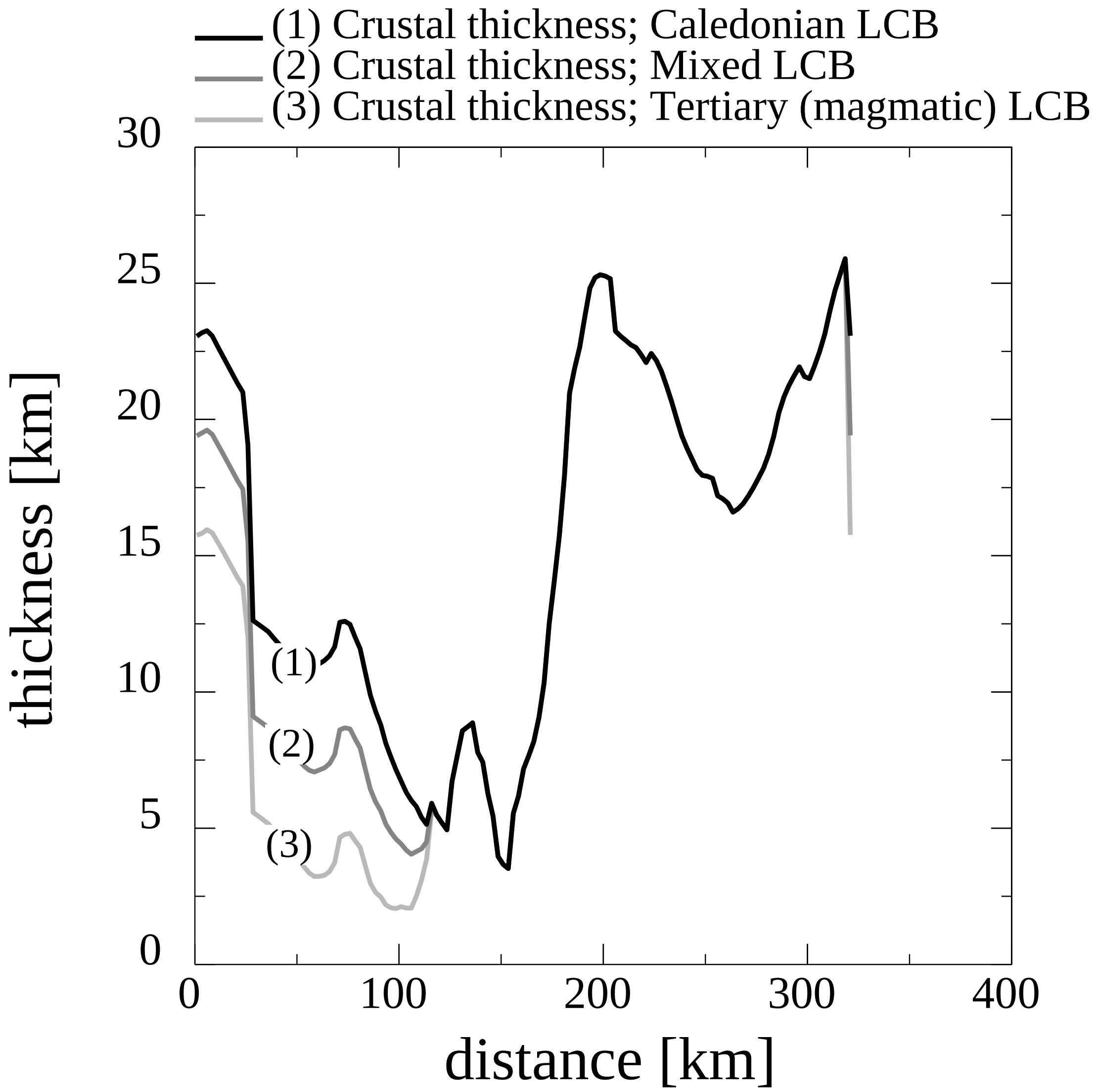

(1) Crustal thickness; Caledonian LCB
(2) Crustal thickness; Mixed LCB
(3) Crustal thickness; Tertiary (magmatic) LCB
30
25
20
15
10
5
0
thickness [km]
(1)
(2)
(3)
0
100
200
300
400
distance [km]

Figure: 4

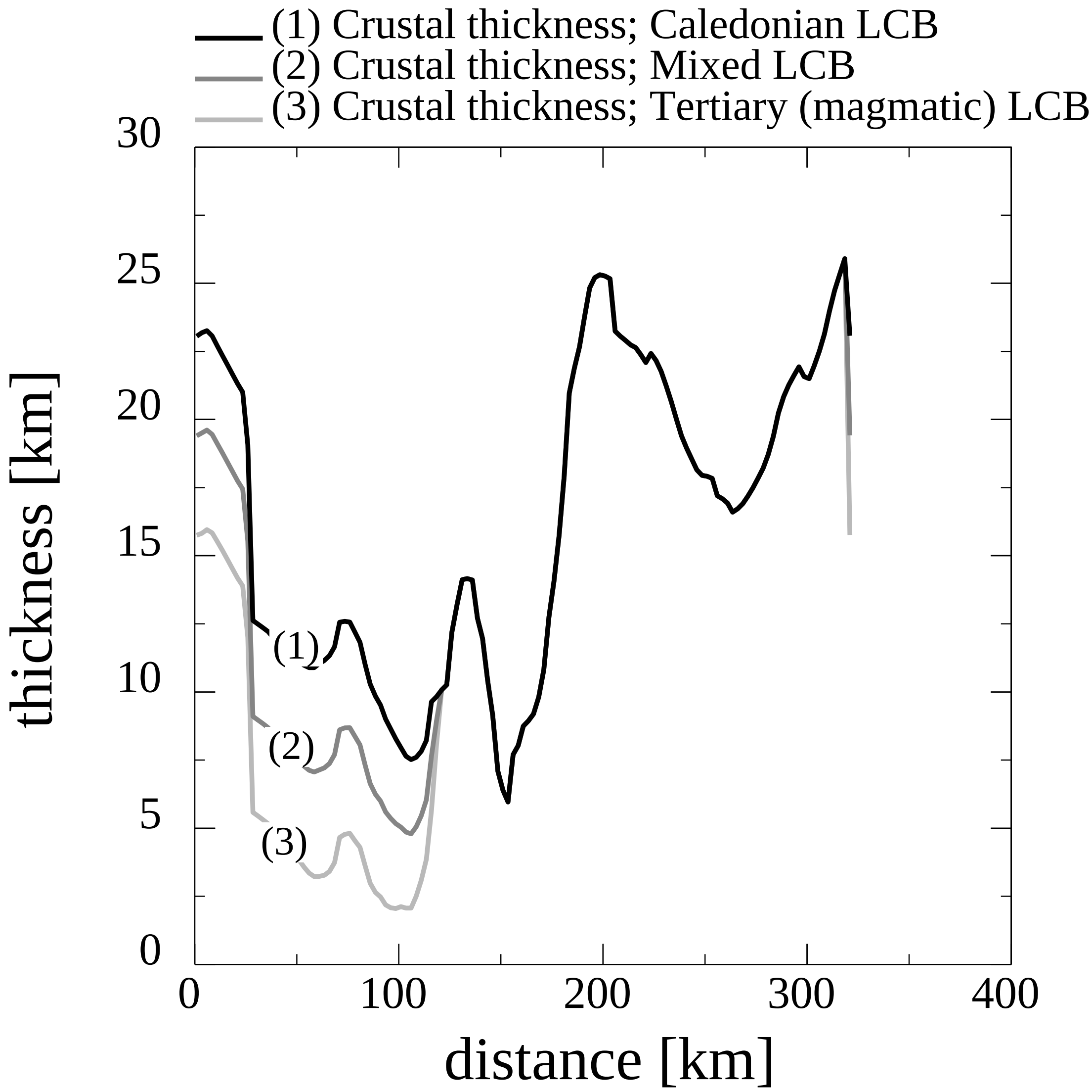
(1) Crustal thickness; Caledonian LCB
(2) Crustal thickness; Mixed LCB
(3) Crustal thickness; Tertiary (magmatic) LCB
thickness [km]
distance [km]
0
5
10
15
20
25
30
0
100
200
300
400
(1)
(2)
(3)

Figure: 5

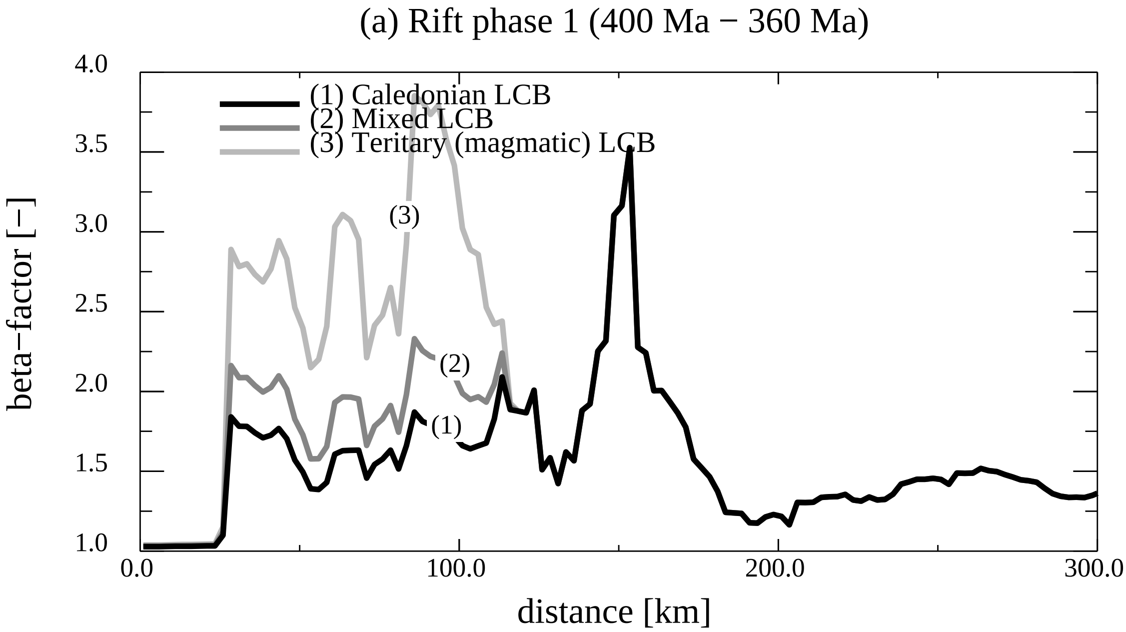
(a) Rift phase 1 (400 Ma − 360 Ma)
(1) Caledonian LCB
(2) Mixed LCB
(3) Teritary (magmatic) LCB
beta−factor [−]
distance [km]
(1)
(2)
(3)

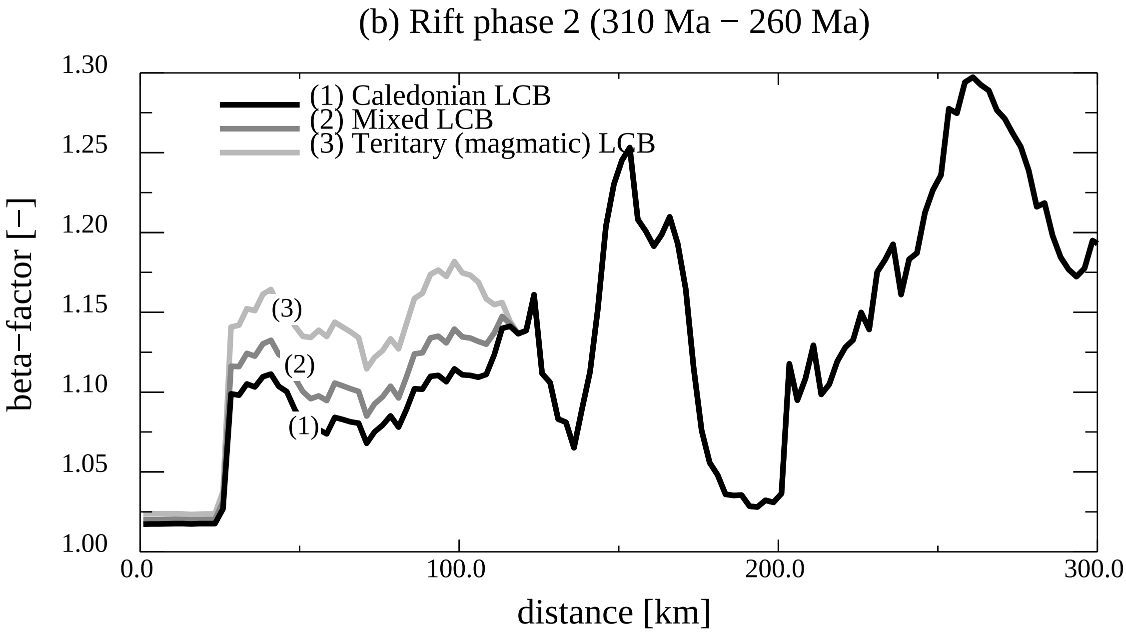
(b) Rift phase 2 (310 Ma − 260 Ma)
(1) Caledonian LCB
(2) Mixed LCB
(3) Teritary (magmatic) LCB
beta−factor [−]
distance [km]
(1)
(2)
(3)

Figure: 6ab

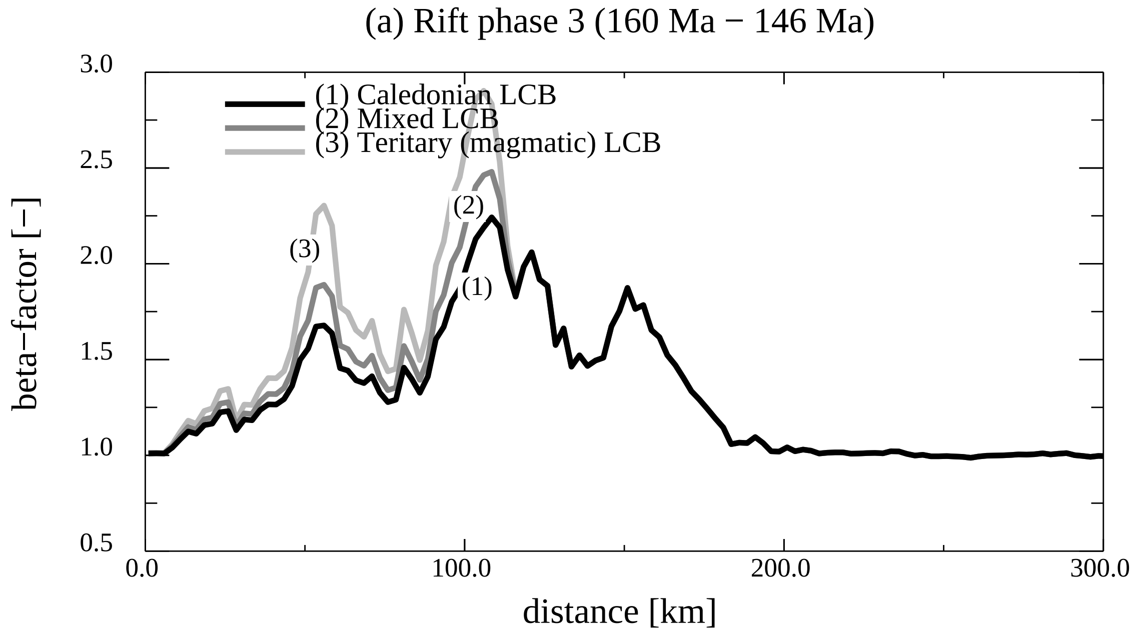

(a) Rift phase 3 (160 Ma − 146 Ma)
(1) Caledonian LCB
(2) Mixed LCB
(3) Teritary (magmatic) LCB
(1)
(2)
(3)
beta−factor [−]
3.0
2.5
2.0
1.5
1.0
0.5
0.0
100.0
200.0
300.0
distance [km]

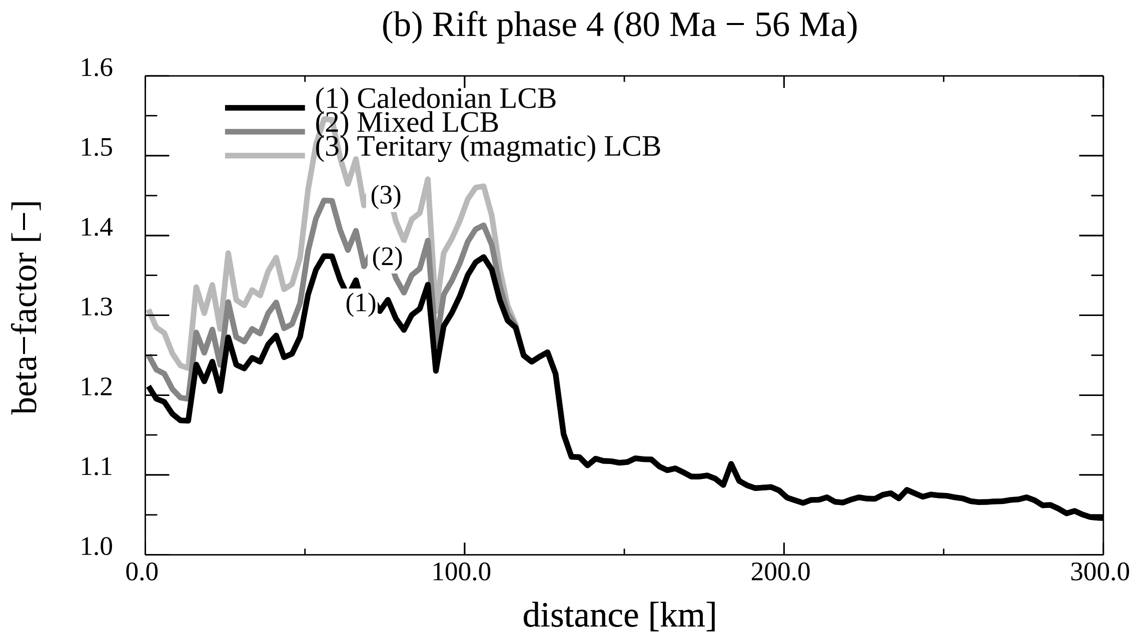

(b) Rift phase 4 (80 Ma − 56 Ma)
(1) Caledonian LCB
(2) Mixed LCB
(3) Teritary (magmatic) LCB
(1)
(2)
(3)
beta−factor [−]
1.6
1.5
1.4
1.3
1.2
1.1
1.0
0.0
100.0
200.0
300.0
distance [km]

Figure: 6cd

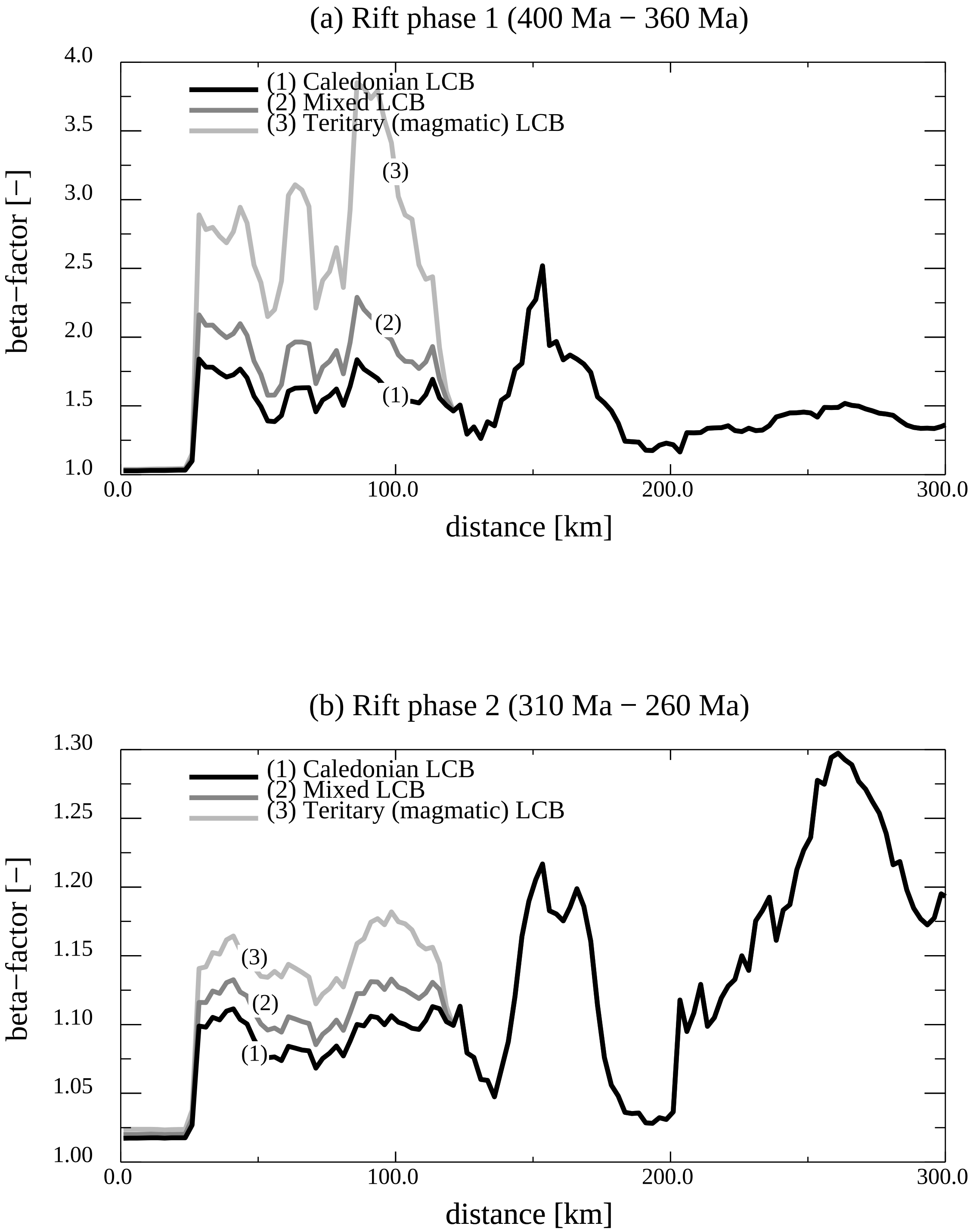
(a) Rift phase 1 (400 Ma − 360 Ma)
(1) Caledonian LCB
(2) Mixed LCB
(3) Teritary (magmatic) LCB
(3)
(2)
(1)
beta−factor [−]
distance [km]
(b) Rift phase 2 (310 Ma − 260 Ma)
(1) Caledonian LCB
(2) Mixed LCB
(3) Teritary (magmatic) LCB
(3)
(2)
(1)
beta−factor [−]
distance [km]

Figure: 7ab

(a) Rift phase 3 (160 Ma − 146 Ma)

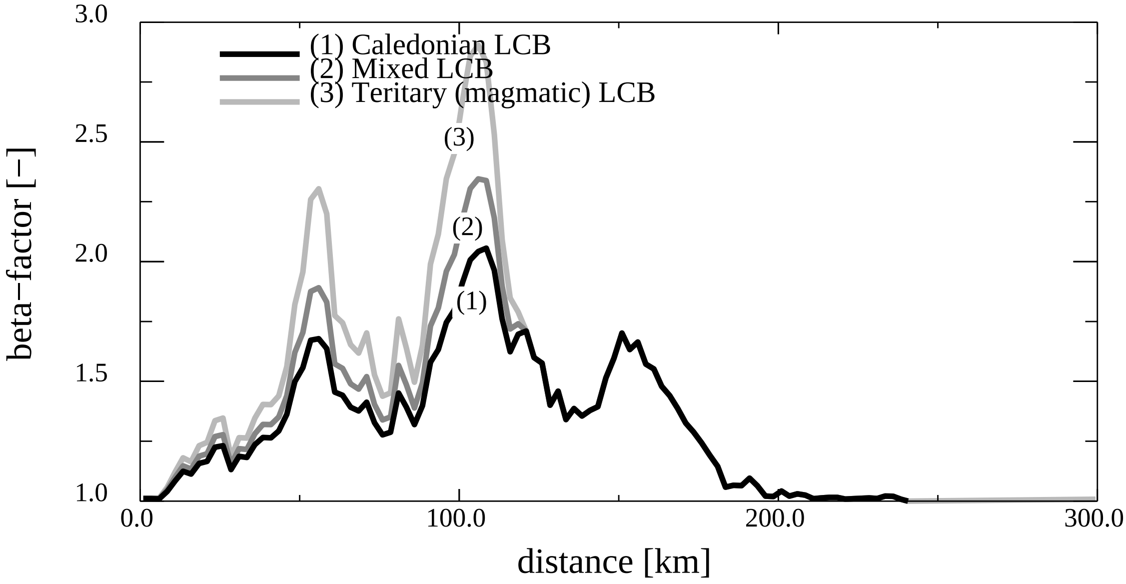

(b) Rift phase 4 (80 Ma − 56 Ma)

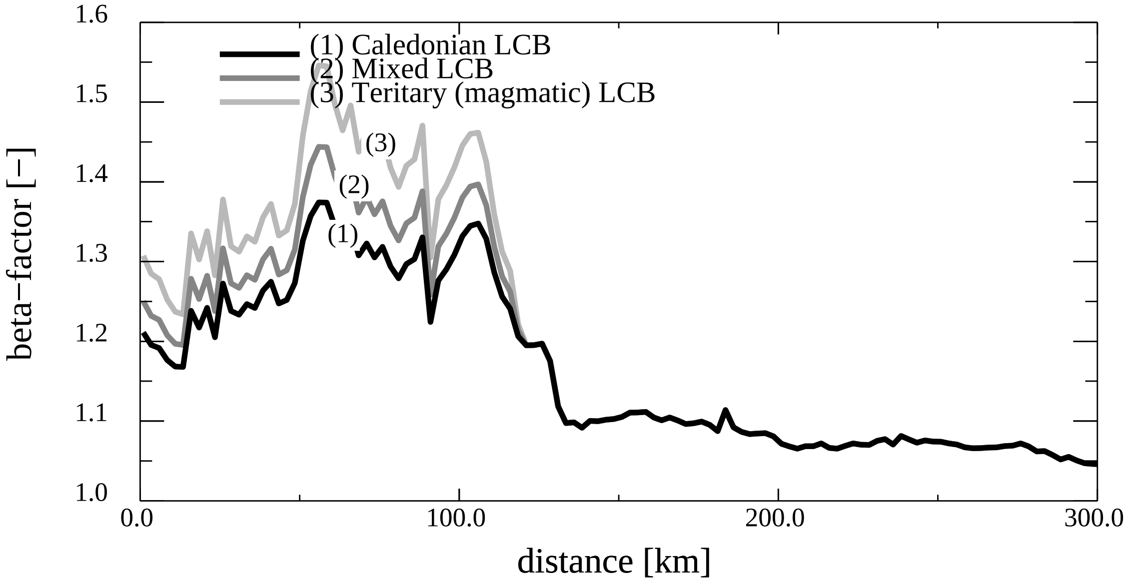

Figure: 7cd

Caledonian LCB

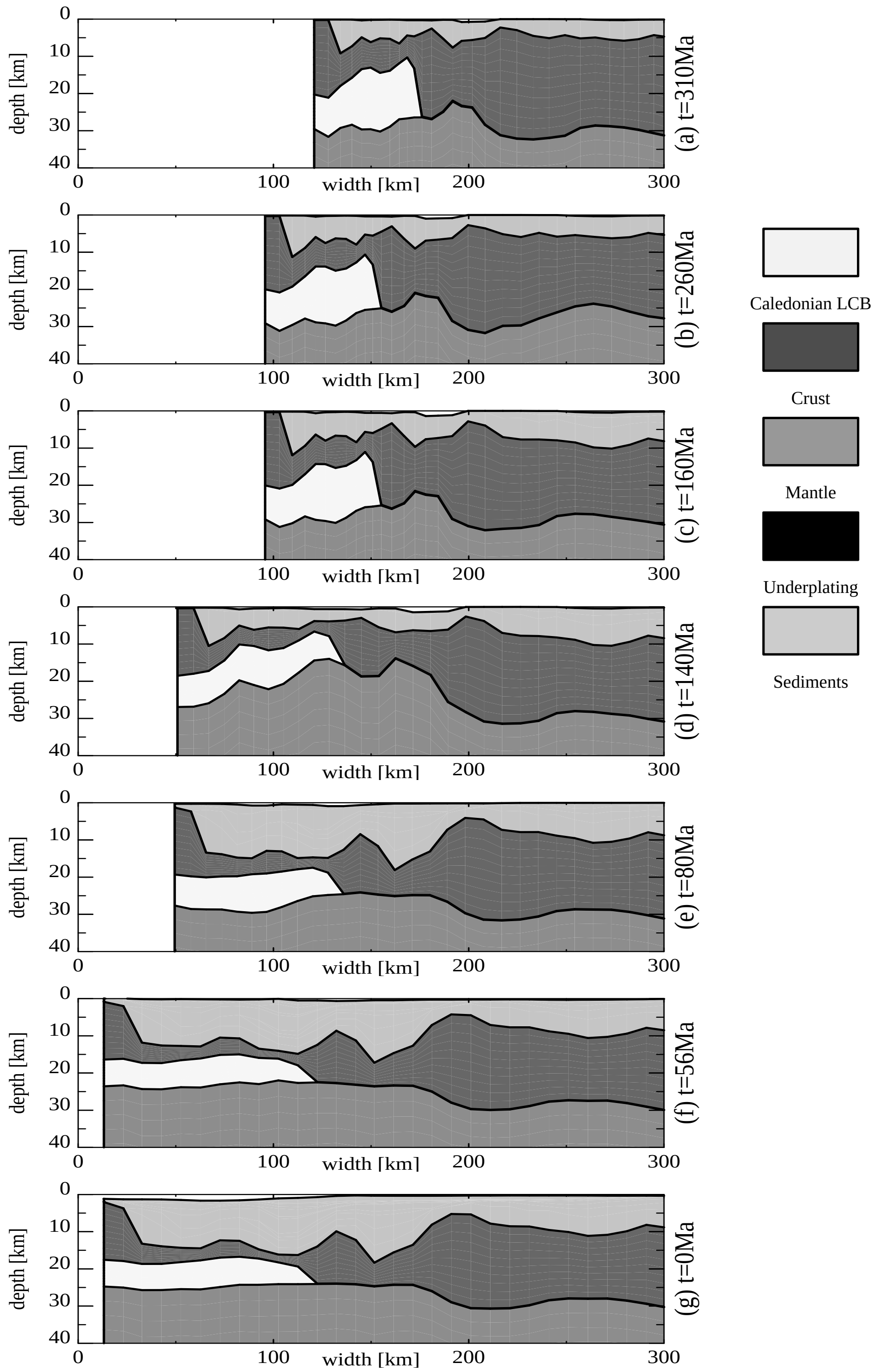

Figure: 8

Mixed LCB

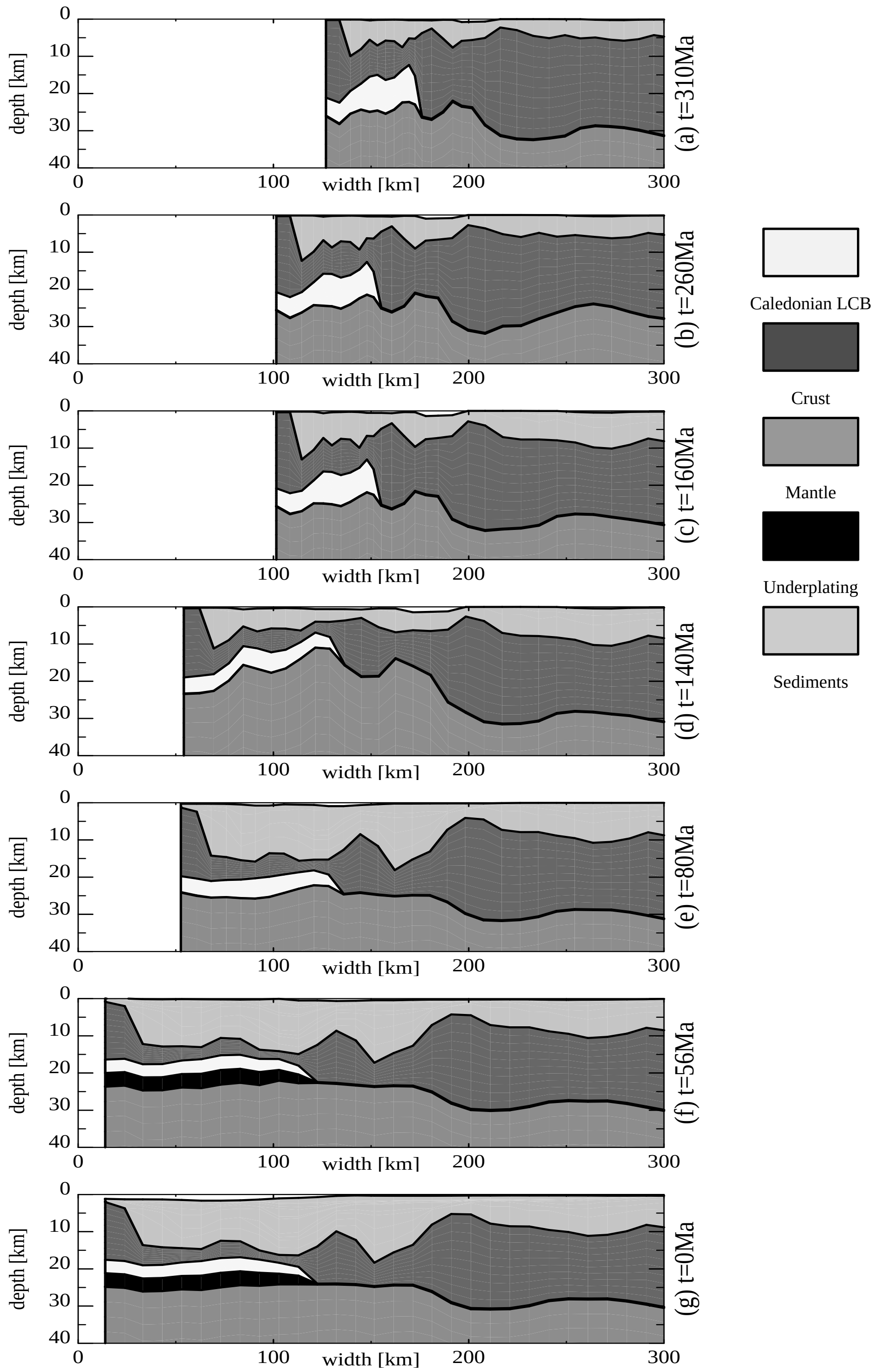

Figure: 9

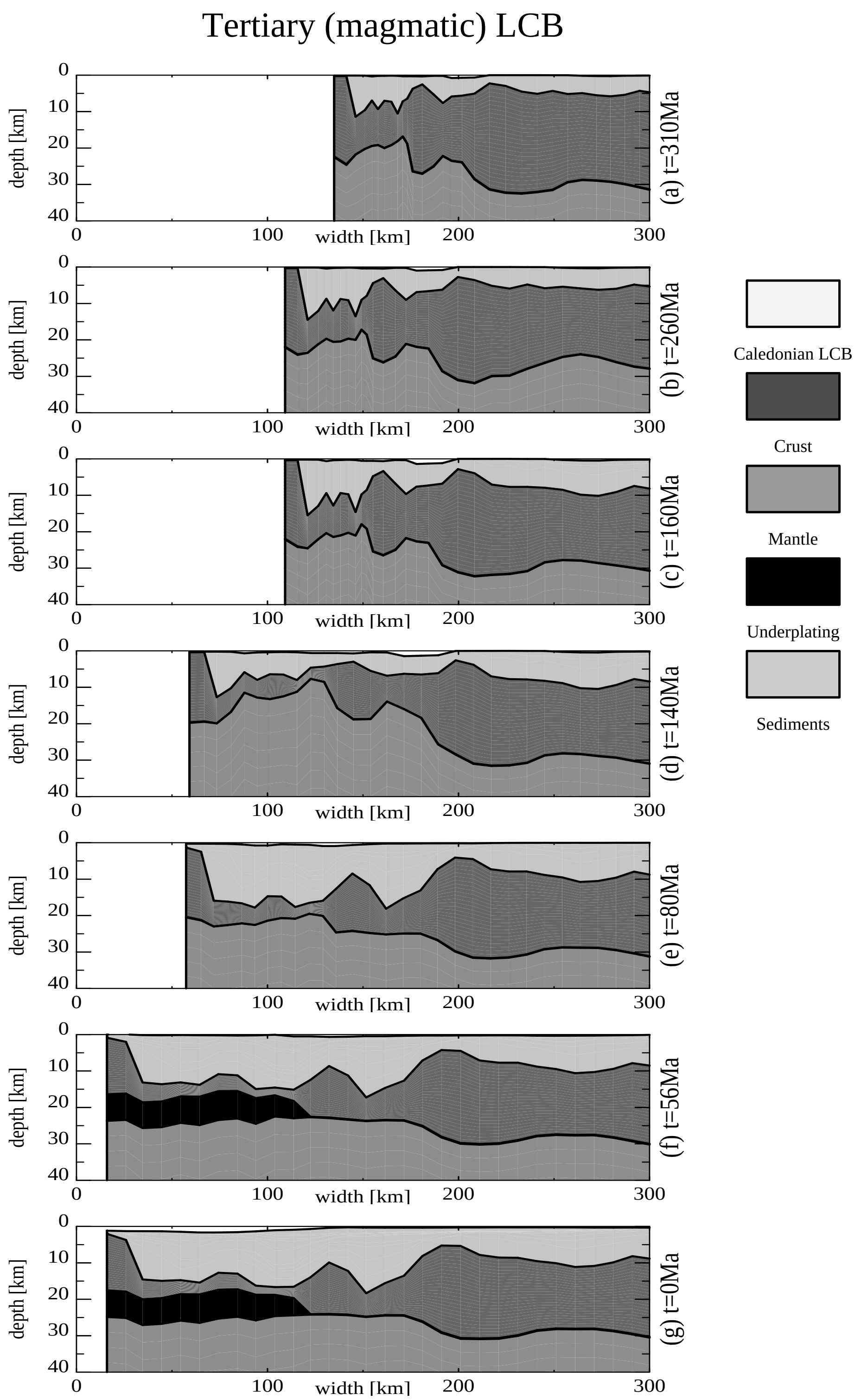
Tertiary (magmatic) LCB
depth [km]
width [km]
(a) t=310Ma
(b) t=260Ma
(c) t=160Ma
(d) t=140Ma
(e) t=80Ma
(f) t=56Ma
(g) t=0Ma
Caledonian LCB
Crust
Mantle
Underplating
Sediments

Figure: 10

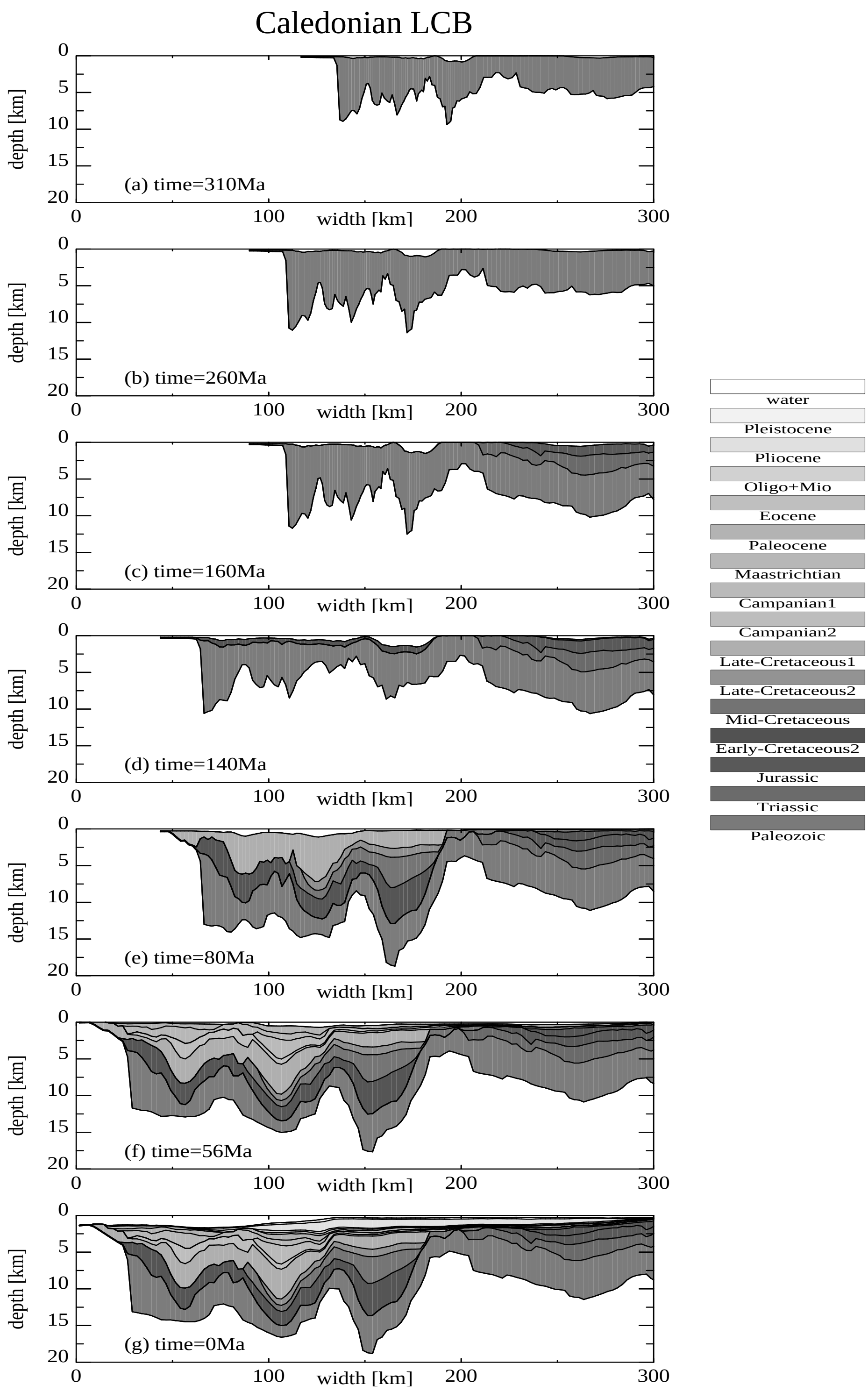
Caledonian LCB
(a) time=310Ma
(b) time=260Ma
(c) time=160Ma
(d) time=140Ma
(e) time=80Ma
(f) time=56Ma
(g) time=0Ma
depth [km]
width [km]
water
Pleistocene
Pliocene
Oligo+Mio
Eocene
Paleocene
Maastrichtian
Campanian1
Campanian2
Late-Cretaceous1
Late-Cretaceous2
Mid-Cretaceous
Early-Cretaceous2
Jurassic
Triassic
Paleozoic

Figure: 11

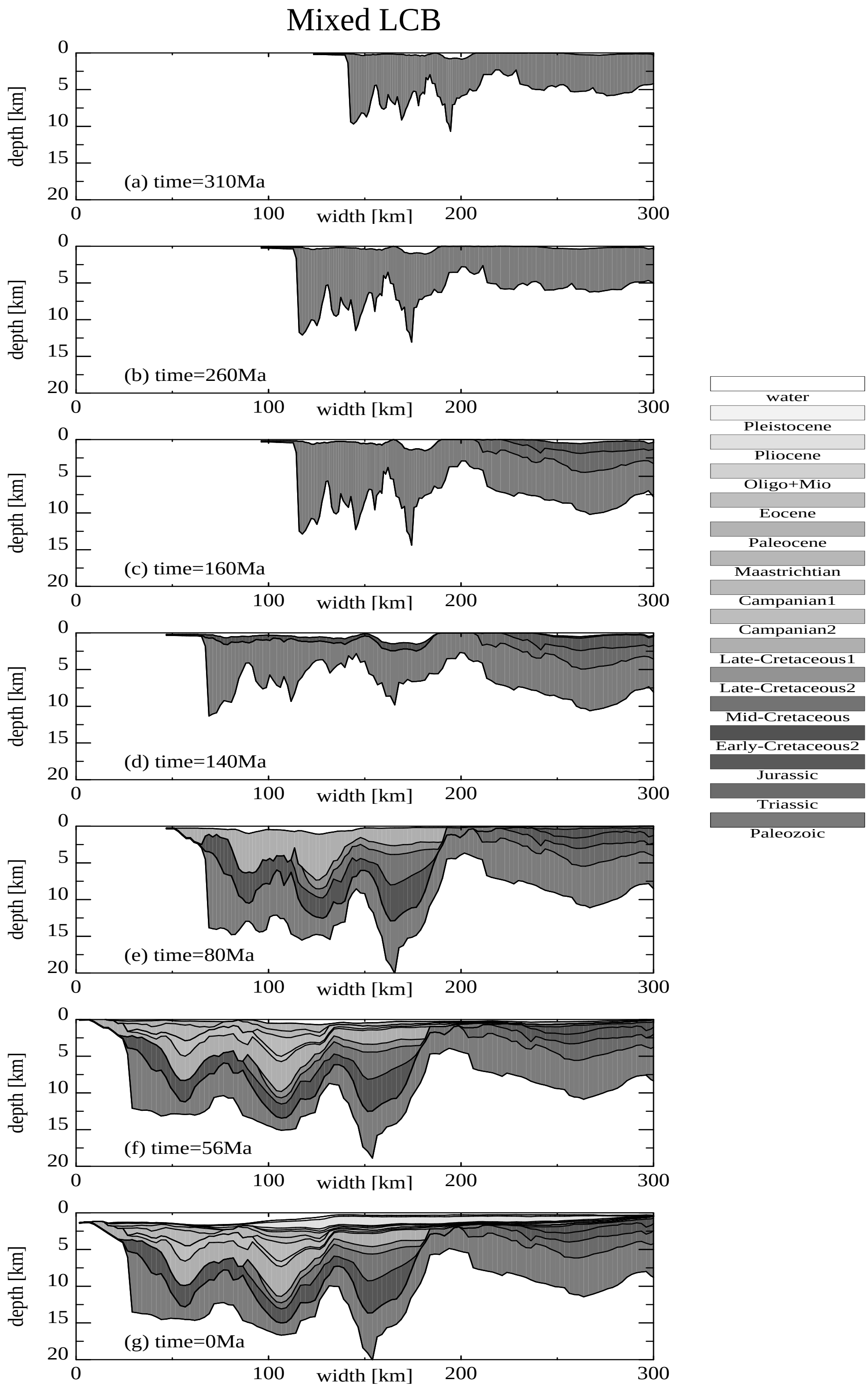

Mixed LCB
depth [km]
width [km]
(a) time=310Ma
(b) time=260Ma
(c) time=160Ma
(d) time=140Ma
(e) time=80Ma
(f) time=56Ma
(g) time=0Ma
water
Pleistocene
Pliocene
Oligo+Mio
Eocene
Paleocene
Maastrichtian
Campanian1
Campanian2
Late-Cretaceous1
Late-Cretaceous2
Mid-Cretaceous
Early-Cretaceous2
Jurassic
Triassic
Paleozoic

Figure: 12

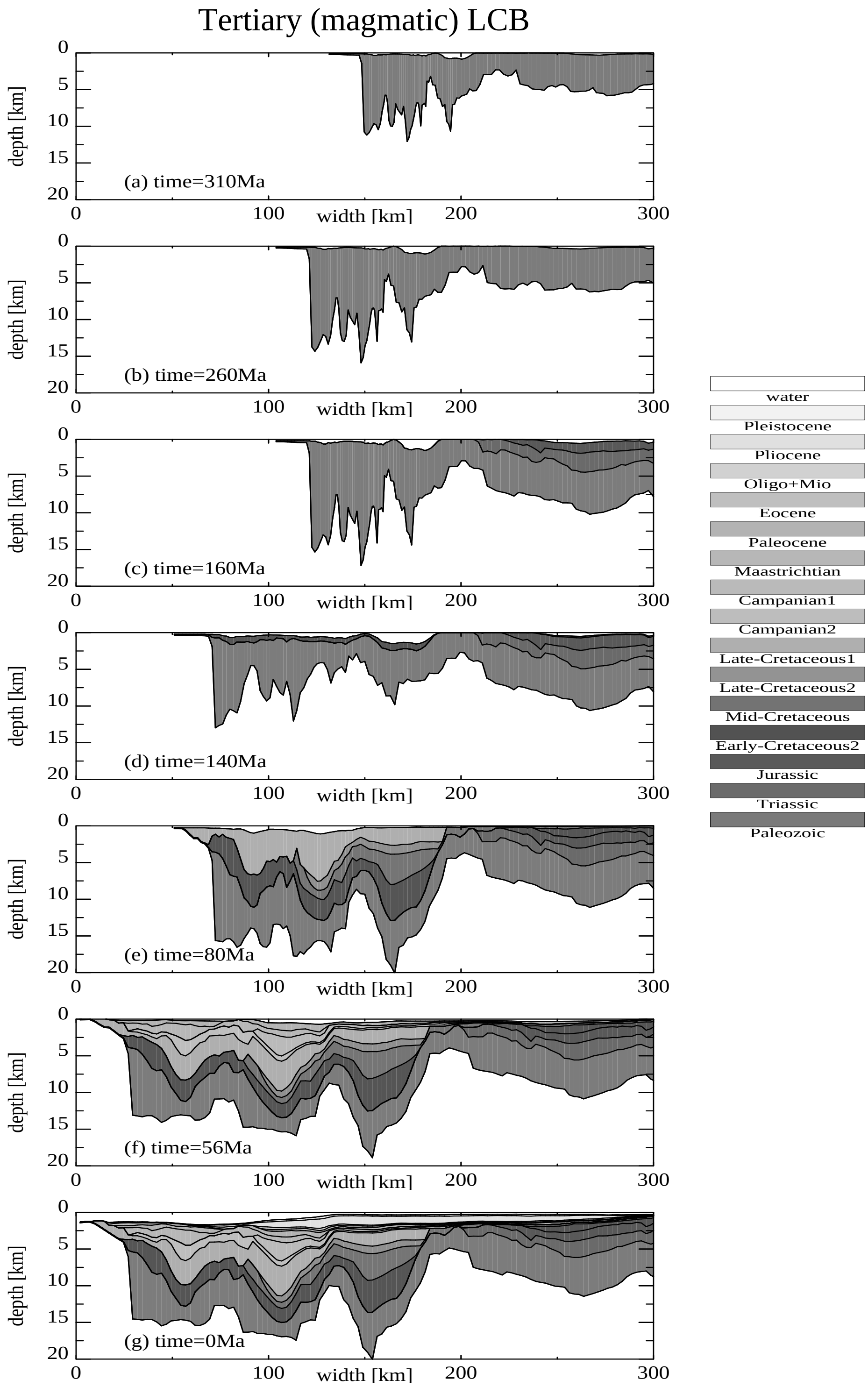

Tertiary (magmatic) LCB
depth [km]
width [km]
(a) time=310Ma
(b) time=260Ma
(c) time=160Ma
(d) time=140Ma
(e) time=80Ma
(f) time=56Ma
(g) time=0Ma
0
5
10
15
20
0
100
200
300
water
Pleistocene
Pliocene
Oligo+Mio
Eocene
Paleocene
Maastrichtian
Campanian1
Campanian2
Late-Cretaceous1
Late-Cretaceous2
Mid-Cretaceous
Early-Cretaceous2
Jurassic
Triassic
Paleozoic

Figure: 13

Institute for Energy Technology

Institute for Energy Technology
P.O. Box 40
NO-2027 Kjeller
Norway
Tlf 0047 63 80 60 00
Telefax 0047 63 81 63 56
www.ife.no